LASER INDUCED DIELECTRIC BREAKDOWN AND MECHANICAL DAMAGE IN SILICATE GLASSES

by

BHIM SAIN SHARMA

SIMON FRASER UNIVERSITY

September 1968

LASER INDUCED DIELECTRIC BREAKDOWN AND MECHANICAL DAMAGE IN SILICATE GLASSES

by

BHIM SAIN SHARMA

B.Sc. (Physics Hons. School) Panjab University (India), 1961

M.Sc. (Physics Hons. School) Panjab University (India), 1962

A DISSERTATION SUBMITTED IN PARTIAL FULFILLMENT

OF THE REQUIREMENTS FOR THE DEGREE OF

DOCTOR OF PHILOSOPHY

in the Department

of

PHYSICS

Simon Fraser University

September 1968

EXAMINING COMMITTEE APPROVAL

(Dr. K. E. Rieckhoff)
Senior Supervisor

(Dr. J. C. Irwin)
Examining Committee

(Dr. K. S. Viswanathan)
Examining Committee

(Dr. M. Hercher)
External Examiner

PARTIAL COPYRIGHT LICENSE

I hereby grant to Simon Fraser University the right to lend my thesis or dissertation (the title of which is shown below) to users of the Simon Fraser University Library, and to make partial or single copies only for such users or in response to a request from the library of any other university, or other educational institution, on its own behalf or for one of its users. I further agree that permission for multiple copying of this thesis for scholarly purposes may be granted by me or the Dean of Graduate Studies. It is understood that copying or publication of this thesis for financial gain shall not be allowed without my written permission.

Title of Thesis/Dissertation:

_____

_____

_____

_____

Author: _____

(signature)

_____

(name)

_____

(date)

ABSTRACT

Dielectric breakdown and mechanical damage in silicate glasses under high intensity laser radiation is investigated in detail. A Q-switched ruby laser is used to induce photoconductivity in soda glass, fused quartz and quartz crystal. The number of charge carriers produced per laser pulse of 10^{27} photons cm^{-2} s^{-1} is accounted for by multiphoton ionization of nonbridging oxygens in the silicon oxygen network. The relative magnitude of the effect proves that the photoconductivity does not result from ionization of sodium in glass as extensively quoted in literature. The lifetime of the charge carriers produced is estimated to be 10^{-5}s.

From thermoelastic considerations a criterion for the validity of possible damage mechanisms is established. It is shown that stimulated Brillouin scattering cannot give rise to an effective absorption of 50 cm^{-1} in the focal volume as required by the thermoelastic considerations. It is proposed and established that the mechanical damage is caused by the acceleration of primary electrons produced by multiphoton ionization, leading to a fully developed electronic instability in few nanoseconds. At this electron density the absorption in the focal volume is 10^{6} cm^{-1}, and is responsible for the complete absorption of the laser pulse at intensities above the threshold for breakdown. The diffusion and recombination of electrons are found to be negligible, the only rate limiting

process being the loss of electron energy to the lattice. The variation in the threshold intensity for breakdown in different glasses is due to the variations in the elastic scattering cross section. The study of the mechanical damage caused by a laser pulse, leads to the estimation of the surface energy of the material, which in the case of soda glass is found to be 10^5 ergs/cm^2. The enhancement of the photoconductivity signal is obtained when a second laser pulse comes within the time 10^{-5}-5 x 10^{-4} sec. of the first pulse. The additional number of electrons produced by the second pulse is accounted for by the ionization of the color centers, caused by trapping the electrons produced by the first pulse.

TABLE OF CONTENTS

		Page
ABSTRACT		iii
LIST OF ILLUSTRATIONS		vii
ACKNOWLEDGEMENTS		viii
CHAPTER I	INTRODUCTION	1
CHAPTER II	THE DAMAGE PHENOMENON	7
CHAPTER III	ENERGY CONSIDERATION FOR DAMAGE IN GLASSES	12
(i)	Mathematical Formulation	13
(ii)	Evaluation of Temperature Field	14
(iii)	Final Wave Equation	17
(iv)	Determination of Stress Field	18
(v)	Estimate of the Effective Absorption Coefficient ξ	19
CHAPTER IV	POSSIBLE MECHANISMS FOR ENERGY CONVERSION	27
(i)	Electrostriction	27
(a)	Direct Light Pressure	28
(b)	Electrostrictive Pressure	28
(ii)	Stimulated Brillouin Scattering	30
CHAPTER V	PHOTOCONDUCTIVITY IN GLASS INDUCED BY Q-SWITCHED RUBY LASER	38
(i)	Historical Sketch	38
(ii)	Experimental Arrangement	40
(iii)	Experimental Results	44
(iv)	Discussion	52
(v)	Multiphoton Ionization	57
(a)	Tunnelling Theory	58
(b)	Perturbation Theory	60
CHAPTER VI	PLASMA FORMATION AND ENERGY ABSORPTION	63
(i)	Classical Microwave Breakdown Theory	66
(ii)	Absorption by Inverse Bremstrahlung	70
(iii)	The effect of initiating electrons and electron multiplication	77
(iv)	Absorption of Radiation in the focal volume	79

CHAPTER VII FURTHER WORK, DISCUSSION AND CONCLUSIONS 84

(i) Enhancement of Photoconductivity 84
(ii) Induced change in refractive index 90
(iii) Estimation of the surface energy of glass 92
(iv) Effect of primary electrons on the breakdown threshold 93
(v) Conclusions 94

APPENDIX I STRUCTURE OF GLASS 96

Transparency of glass 101

APPENDIX II NOTE ON THE STRENGTH OF GLASS 103

APPENDIX III EVALUATION OF THE SCATTERING CROSS SECTION IN GLASS 110

BIBLIOGRAPHY 120

LIST OF ILLUSTRATIONS AND TABLES

Figure		Page
1.	The incident and transmitted laser pulse	16
2.	The radial and hoop stress fields	21
3.	Hoop stresses for two different pulse widths	23
4.	Schematic for observing laser induced photo-conductivity	41
5.	Sample and electrical connections	41
6.	Temperature control, Wheat Stone Bridge	41a
7.	Temperature control, Relay system	41a
8.	Typical laser induced photoconductivity signal	45
9.	Intensity dependence of the induced photoconductivity	45a
10.	Transmission curves for glass and fused quartz	53
11.	Photoconductivity in glass by UV light	74
12.	Schematic for the effect of UV light on laser induced photoconductivity	76
13.	Plot for number of electrons liberated vs incident photon flux, with UV and without UV	77
14.	Typical double pulse photoconductivity signal	85
15.	Schematic for time delaying	86
16.	Typical double pulse signal (time delay $\approx$ 25 ns)	87
17.	Two dimensional structure of quartz crystal, fused quartz and glass	100a

Tables

1.	Damage and stimulated brillouin scattering threshold	36
2.	Time between electron atom collision in glass for different models	119

ACKNOWLEDGMENTS

The research described in this thesis was financed by the National Research Council and Defence Research Board of Canada through the research grants to Dr. K. E. Rieckhoff and the offer of a teaching assistantship by Dr. R. R. Haering which made it possible for the author to come to Simon Fraser University.

I wish to express my sincere gratitude to the following persons who contributed to the success of this work:

Dr. K. E. Rieckhoff as research supervisor, for suggesting this topic and for his helpful guidance throughout the course of this investigation.

Dr. J. C. Irwin for continued interest, encouragement and innumerable helpful discussions which accelerated the completion of this research

Dr. K. S. Viswanathan for reading the manuscript and many helpful suggestions.

Mr. P. A. Barnes and Mr. A. Jmaeff for many useful discussions.

Dr. K. M. S. Sexana for helpful assistance in computer programming.

Mr. J. Mercier and Mr. W. Schneider for drafting and Mrs. E. Waite, Mrs. S. M. Ginetz and Mrs. J. S. Simpson for the neat typing of the thesis.

My wife, Sushi whose sacrifices made all this possible and my son, Bineet for not creating all the troubles he could have.

CHAPTER I

INTRODUCTION

The recent appearance of intense sources of coherent electromagnetic radiation in the optical region has given rise to the study of nonlinear interactions of radiation with matter. One of the phenomena of interest is the breakdown process of solids caused by intense laser radiation and in particular the breakdown of transparent dielectrics. While the basic difficulty in the problem of the breakdown of opaque solids lies in understanding the kinetics of the breakdown, the light absorption mechanism being well known, in the case of transparent materials it is the very act of light absorption and the consequent transfer of this absorbed energy into mechanical energy which is of primary interest.

Destruction of organic and inorganic glasses and of many other transparent dielectrics has been observed by many workers under irradiation by Q-switched as well as non Q-switched ruby laser pulses[1-7]. In the case of non Q-swtiched laser pulses, where the peak power is small but the total energy in the pulse is large, sufficient energy to cause mechanical damage may be absorbed in the focal volume as a consequence of residual linear absorption of the medium in question[8]. For a Q-switched laser pulse, the peak power is many orders of magnitude higher, while the total energy in the pulse is usually very much smaller than in the non Q-switched case and the residual linear absorption is too small to account for the energy removed from the laser

pulse. Here it is the high peak power density which renders the nonlinear interactions between electromagnetic radiation and matter important. The study of the specific nonlinear interactions which lead to a very high absorption of laser radiation within the transparent glasses and the consequent transformation of the absorbed energy into the mechanical energy leading to a destruction of the material is the main subject of this thesis.

Chapter II gives a detailed review of the nature of the destructive effects in silicate glasses where damage occurs typically at ruby laser power densities of 3×10^9 to 5×10^{10} watts/cm^2 depending on the composition, thermal history of the sample as well as the f-number of the focussing lens. Criteria for the validity of the possible nonlinear absorption mechanisms from thermoelastic considerations following the treatment of Conners and Thompson[9] are established in Chapter III. Assuming that the destruction of the material is caused by the thermal stresses set up within the material as a consequence of rapid heating caused by the nonlinear absorption of the laser radiation, it is shown in this thesis that an effective absorption coefficient of at least 50 cm^{-1} in the focal region is required to generate stresses exceeding the strength of the material. From the nature of the thermal stresses generated, some of the features of the mechanical damage are explained. The effect of the pulse duration and the peak powers above the threshold value are also considered.

A review of the possible mechanisms for the laser induced mechanical damage is given in Chapter IV. The generation of an intense hypersonic sound wave by the stimulated Brillouin scattering of the incident laser radiation was first suggested by Chiao, Townes and Stoicheff[10]. Many workers have tried to explain the various aspects of the damage phenomenon using this hypothesis[11,7]. It is shown here that in materials where stimulated Brillouin scattering is observed, it can only account for an effective absorption coefficient of 0.1 cm^{-1}. Also, since damage is observed in materials like CaF_2, MgO etc. where no stimulated Brillouin scattering has been observed, other mechanisms must be considered even in those cases where stimulated Brillouin scattering does occur. In chapters V and VI an alternative damage mechanism is proposed and considered in considerable detail for the first time.

The experimental observation of the laser induced photoconductivity in silicate glasses by Sharma and Rieckhoff[12] is presented in chapter V. Rohatgi[13] in 1957 observed photoconductivity in soda glass and Pyrex using ultraviolet light of wavelength 2537Å, and explained his results as due to the ionization of sodium atoms in a 10Å thick surface layer of glass. Here it is shown that the electrons are in fact liberated by the ionization of the bridging and nonbridging oxygen ions in these glasses by the UV light or by multiphoton absorption of the laser radiation. Using the theory of multiphoton ionization developed by Gold and Bebb[14], the number of free electrons

liberated by a given incident laser pulse has been calculated. An order of magnitude agreement with the experimental results is obtained. Our interpretation of Rohatgi's experiments is also presented. It is further shown for the first time that the multiphoton ionization alone cannot account for the effective absorption required, but merely provides an initiating mechanism and the electrons thus liberated must build up by some multiplicative process to a critical density.

The multiplicative processes leading to a fully developed electronic instability are considered in chapter VI. Here the high frequency laser-induced breakdown and the dielectric breakdown experiments with pulsed d.c. electric fields are compared; the main difference between the two being the mechanism of acceleration of the electrons by the applied electric fields. In the case of d.c. pulsed experiments an average electron picks up sufficient energy during a mean free path so as to cause collisional ionization at the end of a mean free path. While in optical frequency EM fields, electrons absorb photons by the inverse bremstrahlung process[15,16]. The cross section for such an absorption when an electron is scattered by an atom or an ion is calculated from phenomenological considerations[17]. It is shown here that in the case of glass the inverse bremstrahlung cross section in the field of ions is ten times larger than that of atoms. Since the ion density is low in the initial stages of the build up, electrons pick up energy mainly by the absorption of photons in the field of the

atoms and cause collisional ionization. The effect of diffusion and recombination is found to be negligible and the only rate limiting process is the loss of energy of the electrons by elastic collisions with the lattice. At intensities of the incident laser radiation where the rate of gain of energy exceeds the rate of loss of energy, the multiplication of electrons takes place at a very rapid rate and within a few nanoseconds the focal volume is completely ionized. After this stage the free electrons scatter and absorb the incident radiation strongly and can give rise to effective absorption of the order of 10^6 cm^{-1}. This mechanism also explains the strong attenuation of the incident pulse observed when the mechanical damage occurs. Finally, this absorbed energy is transferred to the lattice, and the sudden heating thus caused leads to mechanical fracture.

There were some other novel and interesting experimental observations made during the course of this study:

(i) The surface energy of solid glass can be estimated from the breakdown consideration.

(ii) An enhancement of the photoconductivity signal was observed when a second laser pulse comes within a few milliseconds of the first laser pulse. If the second pulse comes within a few nanoseconds of the first pulse no such enhancement is observed. The presence of light from a high pressure mercury lamp also washed out the enhancement.

(iii) A change in the refractive index of glass at high intensities was observed.

Finally, a summary of the information gained from the experiments as well as a discussion of possible implications and some suggestions for further work in this field are given in chapter VII.

CHAPTER II

THE DAMAGE PHENOMENON

An intriguing aspect of the interaction between light and matter is presented by the phenomenon of damage induced in solids by light of a wavelength at which the material is considered to be transparent. The light in question is usually derived from a high-intensity laser beam such as that produced by a pulsed ruby or neodymium laser. By virtue of the temporal and spatial coherence of these light sources, as evidenced by their monochromatic character and their small beam divergence, they are capable of producing an extremely high power density when focused. Power densities of 10^9 - 10^{11} watts/cm.^{2}, are easily obtained. The many effects observable with such power densities have given rise to new fields of investigation, among them that of laser induced damage in transparent dielectrics.

The damage resistance to laser radiation for different silicate glasses was measured by Cullom and Waynant[2]. Using a Q-switched ruby laser they determined the threshold power density by measuring the maximum power density which can be transmitted without causing visible damage. Their threshold power densities varied from 2×10^9 watts/cm^2 to 7×10^{11} watts/cm^2 for glasses of different chemical composition having different damage threshold. Using their data and comparing it with the information from the manufacturer (Corning Glass Co.) it becomes apparent that the threshold

for damage is dependent on the heat treatment of the glass and on its elastic and thermal properties.

Miller and Boreilli[8] measured the damage threshold for a number of glasses with a non Q-switched ruby laser beam. Here the power densities are much lower than in the Q-switched case and what is determined is the threshold energy. They obtained a range of values from 2.5 to 5 Joule/cm^2 for the threshold and predicted a temperature rise of 1000°C at the center of the focal region within 80 microsecond after the onset of the laser radiation, as the result of the residual linear optical absorption.

Harper[4] irradiated polished pieces of Chance-Pilkington optical glass with a non Q-switched ruby laser beam. Comparing the spectrum of the radiation from the focal region with a black body type continuum, he estimated a temperature rise of 5000°K for an incident laser pulse of 10 Joule energy. This high temperature suggest the formation of a superheated liquid. In the course of his investigations many samples broke apart. Some of the broken samples showed a dark brown or black ring around the actual point of focus and this was attributed to the sudden release of pressure on a superheated liquid, resulting in a small amount of vaporization and subsequent deposition of one or more of the constituent metals or metal oxides.

A similar occurence of high temperatures by focussing a Q-switched ruby laser into glass was first reported by Hercher[1].

Askindaze et al[7] observed that the damage of silicate glasses by a Q-switched ruby laser beam exhibits sharply defined filamentary character. The filaments were markedly thickened in the focal region. The cracks showed no regular orientation away from the focal point and were separated by regions of undamaged material. Near the focus cracks as a rule formed rosettes of planes intersecting along the beam axis. When high energies (2 Joule) per pulse and lenses of shorter focal length ($f < 30$ mm) were used, the nature of the damage changed. Under these conditions cracks formed a large rosette apparently as a result of a point explosion with-in the specimen. The location of the focus with respect to the boundaries of the medium had an effect on the threshold and the nature of the damage. Three types of damage could be identified:

(i) Input interface damage.

This occurs when the beam is focused on the input face. Damage is in the form of shallow conical pits. It is always related to a bright spark. The threshold is low, e.g. of the order of $(2\text{-}5) \times 10^8$ watts/cm^2.

(ii) Output interface damage.

This occurs when the beam is focused on the rear face of the sample. It typically shows as circular conical pits, few tenths of millimeters across and deep. It is not always accompanied by a spark. The threshold is about twice that of type (i).

(iii) Internal damage.

This is the one which is most frequently reported and

occurs when the beam is focused within the sample. The fractures obtained at power densities just above the threshold are generally composed of one or several small discs 0.01 to 1 mm in diameter. The thresholds are higher than for the types (i) and (ii) and range from 5×10^9 watts/cm^2 to 7×10^{11} watts/cm^2 for glasses of different composition. In samples which are longer than the self focussing length of the laser beam, the damage appears as a combination of gross fracture and a long thin filament made up of very small bubbles, extending along the lens axis.

A separate damage phenomenon observed by Giuliano[11] will not be treated here. It occurs when glass shows additional splitting of the rear face of the sample. In his experiments light was passed through a totally internally reflecting roof top prism, being reflected twice before leaving the prism. Damage spots occured not only where the light left the prism but also at the points where it was reflected inside.

Frechette and Cline[18] explored the possibility that the state of polarization of the beam might be of importance in generating the damage, especially within strongly anisotropic materials. They focused an unpolarized beam in a calcite crystal, travelling perpendicular to the rhombohedral cleavage plane in calcite. It was found in a number of trials that the extra-ordinary and ordinary rays caused damage of identical severity. All these experiments confirmed the existence of a critical intensity of the Q-switched laser beam and a critical energy of the non Q-switched beam which must be reached before noticable

damage occurs. Multiple irradiation of the glass samples below the critical intensity at intervals of 2 to 3 minutes does not cause any visible damage.

In summary then, we may describe the damage phenomenon as follows:

The focused beam from a non Q-switched ruby laser heats up the material to temperatures as high as 5000°K., presumably as a consequence of the linear optical absorption in some glasses such as corning number 1723, 7740, 0580 and X95DTA[8]. In the interaction of the Q-switched ruby laser beam with glasses, internal and surface damage occurs. Bubble formation and incandescence indicate that here also high temperatures are involved. Open cracks and cavities inside the bulk of the glasses indicate yielding to the action of high mechanical stresses. The fact that extraordinary and the ordinary rays in calcite are equally damaging, although the directions of their electric field vectors correspond to different packing densities and bonding strengths, implies that no direct coupling occurs between the atoms or ions and the electric field of the beam.

CHAPTER III

ENERGY CONSIDERATION FOR DAMAGE IN GLASSES

Considering the nature of the damage it appears likely that nonlinear absorption processes play an important role in the transfer of energy from the laser beam to the solid. The problem will now be formulated in terms of dynamic thermoelastic theory with a view to determine how much energy must be absorbed from the laser beam by such nonlinear processes to cause a fracture. The energy absorbed from the laser beam is represented by a heat source with a specified space and time dependence. The thermelastic field equation is then solved for the stress distribution. A fundamental assumption used in deriving the equations for the fracture is that the fracture develops after the laser pulse is over[19]. By introducing a criterion for maximum stress fracture resistance under application of a thermal shock, conditions for which the fracture can be initiated during the irradiation process are obtained. All of the absorption processes are represented by a single parameter which may be looked upon as a measure of the average absorption. It is assumed that no significant absorption occurs outside the focal region which is assumed to be a sphere having a diameter equal to a few Airy disk diameters. All of the energy in the laser beam is assumed to enter this region. The approach used here is approximate but can provide some insight into how large the nonlinear effects must be in order to account for the observed damage phenomena.

Mathematical Formulation

This problem has been formulated and investigated in detail by Conners and Thompson[9]. We present here, for the sake of completeness their treatment with some modification of pulse width and fracture criterion. In the absence of body forces, the thermoelastic wave equation in terms of the displacement u_i is[20]:

$$\mu \frac{\partial^2 u_i}{\partial x_i^2} + (\lambda + \mu) \frac{\partial^2 u_k}{\partial x_k \partial x_i} - \beta \frac{\partial T}{\partial x_i} - \rho \frac{\partial^2 u_i}{\partial t^2} = 0 \qquad (1)$$

where λ and μ are Lame's constants, ρ is the mass density and $\beta = (3\lambda + 2\mu)\,\alpha$, α being the coefficient of linear thermal expansion. The temperature field is represented by T. Conventions of tensor analysis such as summation over like indices apply. Assuming that the energy of the focussed laser beam is absorbed in a spherically symmetric region about the focal point of the beam the problem can be expressed in spherical coordinates (r, θ, φ). Under the assumed spherical symmetry, the displacement components u_i are derivable from a scalar potential Φ as follows

$$u_i = \frac{\partial \Phi}{\partial x_i} \qquad (2)$$

With this assumption, the thermoelastic wave equation is

$$\frac{\partial}{\partial x_i}\left[\frac{\partial^2 \Phi}{\partial x_k^2} - \left(\frac{\beta}{\lambda+2\mu}\right) T - \left(\frac{\rho}{\lambda+2\mu}\right) \frac{\partial^2 \Phi}{\partial t^2}\right] = 0 \qquad (3)$$

Integrating (3) and setting the constant of integration (i.e. the ambient temperature) equal to zero;

$$\nabla^2\Phi - \frac{1}{c^2}\frac{\partial^2\Phi}{\partial t^2} = \frac{\beta T}{(\lambda+2\mu)} \quad , \tag{4}$$

where $c^2 = \frac{\lambda + 2\mu}{\rho}$; c being the dilational wave velocity.

Evaluation of temperature field T $(\vec{r}, t)$

Since the laser induced temperature field is the driving function for the thermoelastic waves, we use an uncoupled theory so that the rate of strain tensor does not appear in the energy equation. Thus the temperature field is expressed in terms of the absorbed laser energy through the heat conduction equation:

$$\gamma\nabla^2 T + q = C\frac{\partial T}{\partial t} \tag{5}$$

where q represent the volume heat source and C is the heat capacity, considered to be constant. Assuming the heat conduction to be negligible, because of the low coefficient of the heat conduction and the short times involved, we may set $\gamma\nabla^2 T = 0$. The quantity q is linked to the intensity I of the incident radiation by the equation

$$q = \xi I = C\frac{\partial T}{\partial t} \tag{6}$$

where I is energy flux per unit area, and ξ is the equivalent linear absorption (in cm^{-1}) including the effects of all non-linear absorption processes. On the basis of the diffraction

theory it seems reasonable to approximate the intensity of the laser radiation in the region of the focal point by the spherically symmetric function:

$$I(r,t) = I_0 f(t) \left(\frac{\sin vr}{vr}\right)^2 \tag{7}$$

where $v = \frac{2\pi a}{\lambda_1 f}$ is the lens parameter, a- the aperture radius of the lens, f- its focal length and λ_1 is the wave-length of the ruby laser. The time dependence is determined by the laser pulse shape. Disregrading the initial part of the pulse when absorption is negligible, (see Fig. 2.1) this time dependence can be approximated by a cosine function. Argument of the cosine function is held within the limits $0 \leq \omega t \leq \pi/2$.

Thus in terms of the approximated space and time dependence the equation for the radiation intensity is

$$I = I_0 \left(\frac{\sin vr}{vr}\right)^2 \cos \omega t \; ; \quad 0 \leqslant \omega t \leqslant \frac{\pi}{2} \tag{8}$$

Using (7) and (8) in (6) the expression for $T(\vec{r}, t)$ is

$$C \frac{\partial T}{\partial t} = I_0 \xi \left(\frac{\sin vr}{vr}\right)^2 \cos \omega t \; . \tag{9}$$

Integrating (9) and setting the constant of integration (the ambient temperature) equal to zero, we get:

$$\begin{aligned} T &= \frac{I_0 \xi}{\omega C} \left(\frac{\sin vr}{vr}\right)^2 \sin \omega t \\ &= T_0 \left(\frac{\sin vr}{vr}\right)^2 \sin \omega t \end{aligned} \tag{10}$$

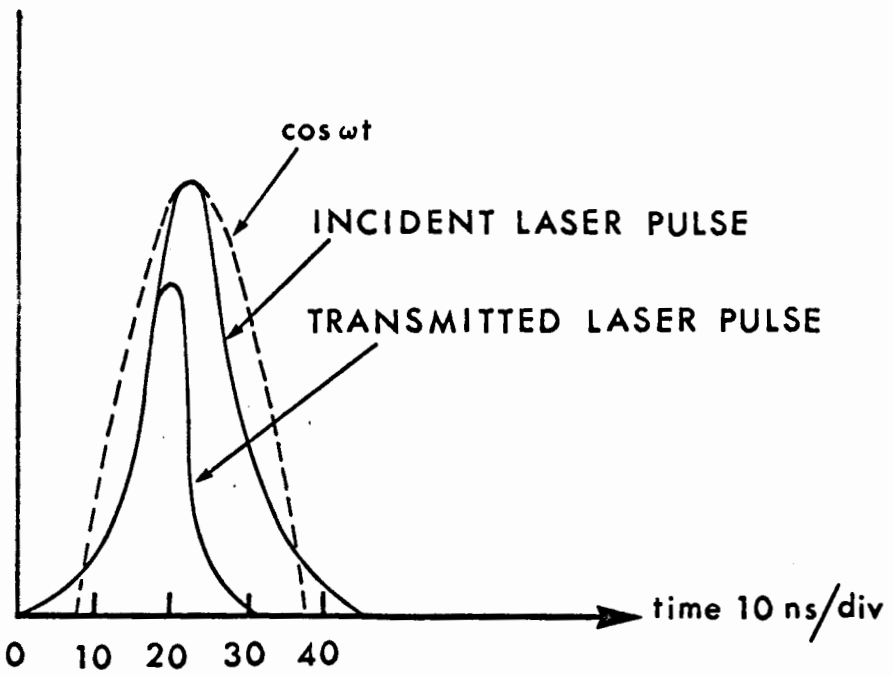
cos ωt
INCIDENT LASER PULSE
TRANSMITTED LASER PULSE
time 10 ns/div
0
10
20
30
40

Fig. 2.1

where $T_0 = \frac{I_0 \xi}{\omega C}$.

The peak intensity $I(0, 0) = I_0$, can be expressed in terms of the peak pulse energy flux E_p as:

$$I_0 = \frac{\pi a^2}{\lambda_1^2 f^2} E_p \tag{11}$$

Now the total pulse energy $Q_T = \int_0^{\pi/2\omega} E \, dt$ where $E = E_p \cos \omega t$.

Thus $Q_T = \frac{E_p}{\omega}$ or $T_0 = \frac{\xi}{\omega C} \cdot \frac{\pi a^2}{\lambda_1^2 f^2} \omega Q_T$

$$T_0 = \frac{V^2 \xi}{4\pi C} Q_T \tag{12}$$

Final wave equation

Substituting into (4) the form of the temperature field

$$\nabla^2 \Phi - \frac{1}{c^2} \frac{\partial^2 \Phi}{\partial t^2} = \frac{\beta T_0}{(\lambda + 2\mu)} \left(\frac{\sin Vr}{Vr} \right)^2 \sin \omega t . \tag{13}$$

To solve this we make the assumption that the scalar potential has the same time dependence as the driving temperature field.

$$\Phi(r, t) = \phi(r) \sin \omega t \tag{14}$$

With this equation (13) can be written as

$$\nabla^2 \phi + k^2 \phi = \frac{\beta T_0}{(\lambda + 2\mu)} \left(\frac{\sin Vr}{Vr} \right)^2 \tag{15}$$

where $k = \frac{\omega}{c}$

Conners and Thompson solved this wave equation using Green's function, under the assumption that the region directly affected by the laser pulse is small as compared to the total dimensions of the sample. They obtained the following expression for the scalar potential:

$$\Phi = \frac{-\beta \xi k^2 Q_T}{4\pi C} \left[M \frac{\cos x}{x} + N \frac{\sin x}{x} \right] \sin \omega t . \qquad (16)$$

where

$$M = \frac{1}{4} \left[2\,Si(x) - Si(2n+1)x - Si(1-2n)x \right] \qquad (17)$$

and

$$N = \frac{1}{4} \left[Ci(1-2n)x + Ci(1+2n)x - 2Ci(x) \right] \qquad (18)$$

$x = kr$ and $n = \frac{v}{k}$; $Si(x)$ and $Ci(x)$ are the sine and cosine integrals.

Determination of the Stress field

From equation (2) the displacements are

$$u_1 = \frac{\partial \Phi}{\partial r} \quad ; \quad u_2 = u_3 = 0 \qquad (19)$$

and the strains are given by

$$\epsilon_{11} = \frac{\partial^2 \Phi}{\partial r^2} \qquad (20)$$

$$\epsilon_{22} = \epsilon_{33} = \frac{1}{r}\frac{\partial \Phi}{\partial r}$$

$$\epsilon_{ij} = 0 \quad \text{for} \quad i \neq j \tag{21}$$

The stresses in terms of the strains are

$$\tau_{ij} = \lambda \epsilon_{ii} \delta_{ij} + 2\mu \epsilon_{ij} - \beta T \delta_{ij} \tag{22}$$

So we have by substituting equations (16)-(21) into (22):

Radial Stress

$$\tau_{11} = \frac{\beta \xi k^2 Q_T}{4\pi C}\left\{M\left[\frac{\cos x}{x} - \frac{4\mu}{\lambda+2\mu}\left(\frac{\sin x}{x^2} - \frac{\cos x}{x^3}\right)\right] + N\left[\frac{\sin x}{x} + \frac{4\mu}{\lambda+2\mu}\left(\frac{\cos x}{x^2} - \frac{\sin x}{x^3}\right)\right]\right\} \sin \omega t . \tag{23}$$

Hoop stresses in the tangential direction:

$$\tau_{22} = \tau_{33} = \frac{\beta \xi k^2 Q_T}{4\pi C}\left\{-\frac{2\mu}{\lambda+2\mu}\left(\frac{\sin nx}{x}\right)^2 + M\left[\frac{\lambda}{\lambda+2\mu}\frac{\cos x}{x} + \frac{2\mu}{\lambda+2\mu}\left(\frac{\sin x}{x^2} + \frac{\cos x}{x^3}\right)\right] + N\left[\frac{\lambda}{\lambda+2\mu}\frac{\sin x}{x} - \frac{2\mu}{\lambda+2\mu}\left(\frac{\cos x}{x^2} - \frac{\sin x}{x^3}\right)\right]\right\} \sin \omega t . \tag{24}$$

Estimate of the effective absorption coefficient

To estimate the minimum amount of absorption required to cause mechanical breakdown, we use the experimental values of Budin and Raffy[3]. For convenience we write the stresses in glass as

$$\tau_{11} = \frac{\beta Q_T \xi}{4\pi C} F(n,x) \sin \omega t$$

$$\tau_{22} = \tau_{33} = \frac{\beta Q_T \xi}{4\pi C} G(n,x) \sin \omega t \qquad (25)$$

where F(n, x) and G(n, x) are given by (23) and (24). Budin and Raffy's[3] experimental results indicate that the threshold for the fracture in Borosilicate glass, free of any platinum inclusions is just above 3×10^9 W/cm^2 or 90 J/cm^2. For a Q-switched ruby pulse of 30 n sec focused by an f/10 lens, the relevant parameters are:

$$\omega = \frac{\pi}{2 \times \text{pulse width}} = \frac{\pi}{2.2 \times 10^{-8}} = 7.85 \times 10^7 \text{ sec}^{-1}$$

Q_T = Total energy in the pulse

$= 5.13 \times 10^{-3}$ Joule

$= 1.22 \times 10^{-3}$ Cal.

$k = \frac{\omega}{c} = 139 \text{ cm}^{-1}$.

where c is the dilational velocity in Borosilicate glass;

$c = 5.64 \times 10^5$ cm/sec

v = lens parameter $= \frac{\pi 2a}{\lambda_1 f} = 9 \times 10^3 \text{ cm}^{-1}$.

$n = \frac{v}{k} = 65$

$\beta = (3\lambda + 2\mu)\alpha = 16.7$ psi/c$^\circ$

$C = 0.446$ cal/cm^3 c$^\circ$

Since there will be a maximum in the temperature gradient at the edge of the illuminated region we calculate the value of G(n,x) at the edge of this region. Thus calculating the value ξ by

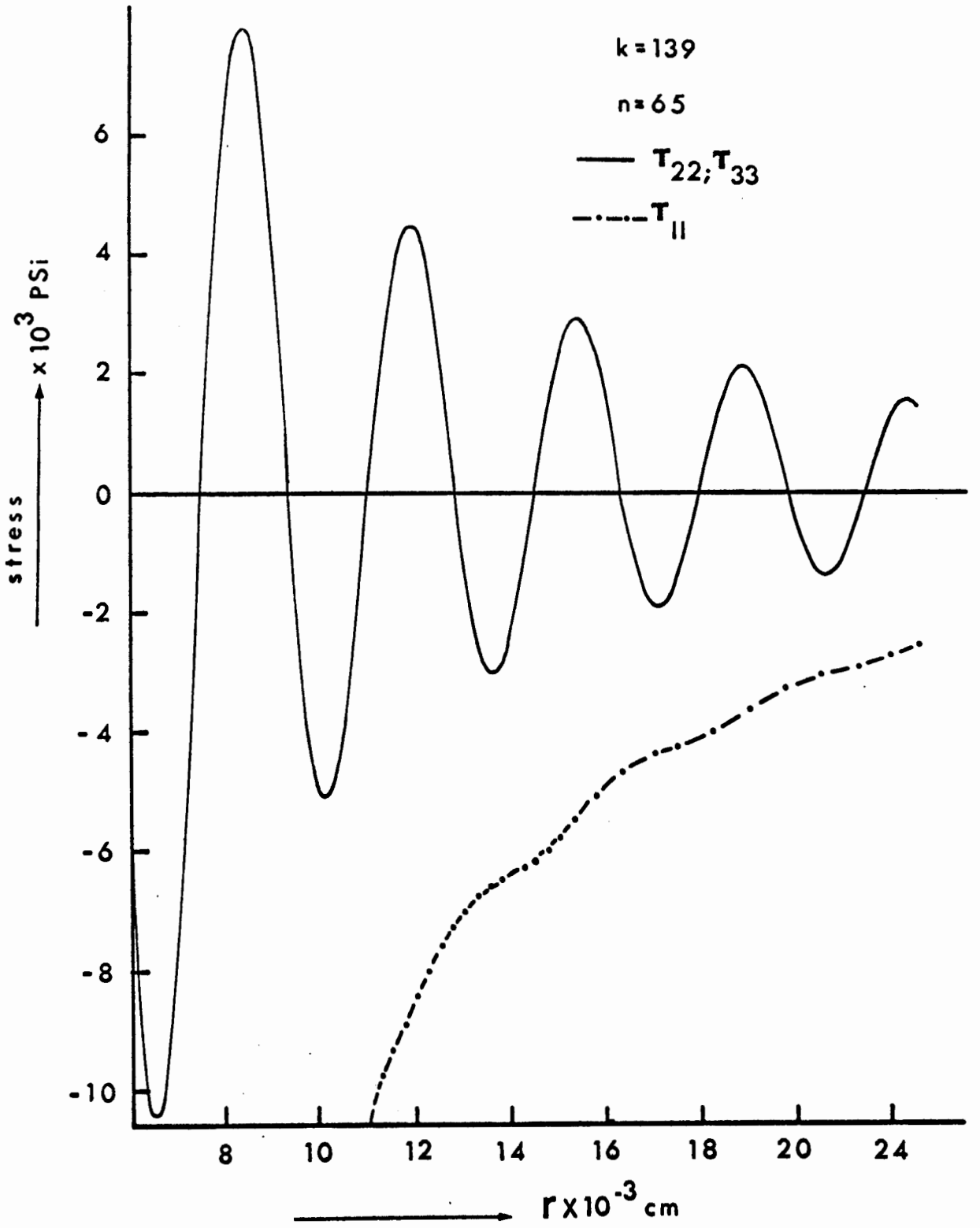
k = 139
n = 65
$T_{22}; T_{33}$
T_{11}
stress $\times 10^3$ PSi
6
4
2
0
-2
-4
-6
-8
-10
8
10
12
14
16
18
20
24
r X 10^{-3} cm

Fig. 2.2

taking the stress τ_{22} equal to the thermal shock resistance of Borosilicate glass (Appendix II).

$$5800 = \frac{\beta Q_T \xi}{4\pi C} \times 3.24 \times 10^3.$$

$$\xi \backsimeq 50 .$$

Using this value of ξ and $Q_T = 6.8 \times 10^{-3}$ Joule for an intensity above threshold, the stress field is plotted using an IBM 360 computer system. Figure 2.2 is a plot of the radial stress τ_{11} and the hoop stress τ_{22} vs the distance from the focal point. Radial stress is compressive and is a monotonically decreasing function of distance from the focal point. The hoop stresses are oscillatory in nature and become compressive and tensile periodically as we move away from the focal point. The amplitude of these oscillations decreases with increasing distance from the focal point. Even though the radial stresses are twice as high as the hoop stresses, it will not damage the glass, since the glasses are known to be much stronger under compression than under tension (Appendix I), the compressive strength of glasses is at least 10 times higher than the tensile strength. Thus the fracture is initiated at the tensile peaks of the stress where the peak amplitude exceeds the tensile strength.

Figure 2.3 shows the effect of the pulse width on the hoop stresses. The full line curve is for the case when the pulse duration is 30 n sec. The dotted curve is for the case when the initial part of the pulse is not considered and the pulse duration is 20 n sec but has the same total energy. Peak

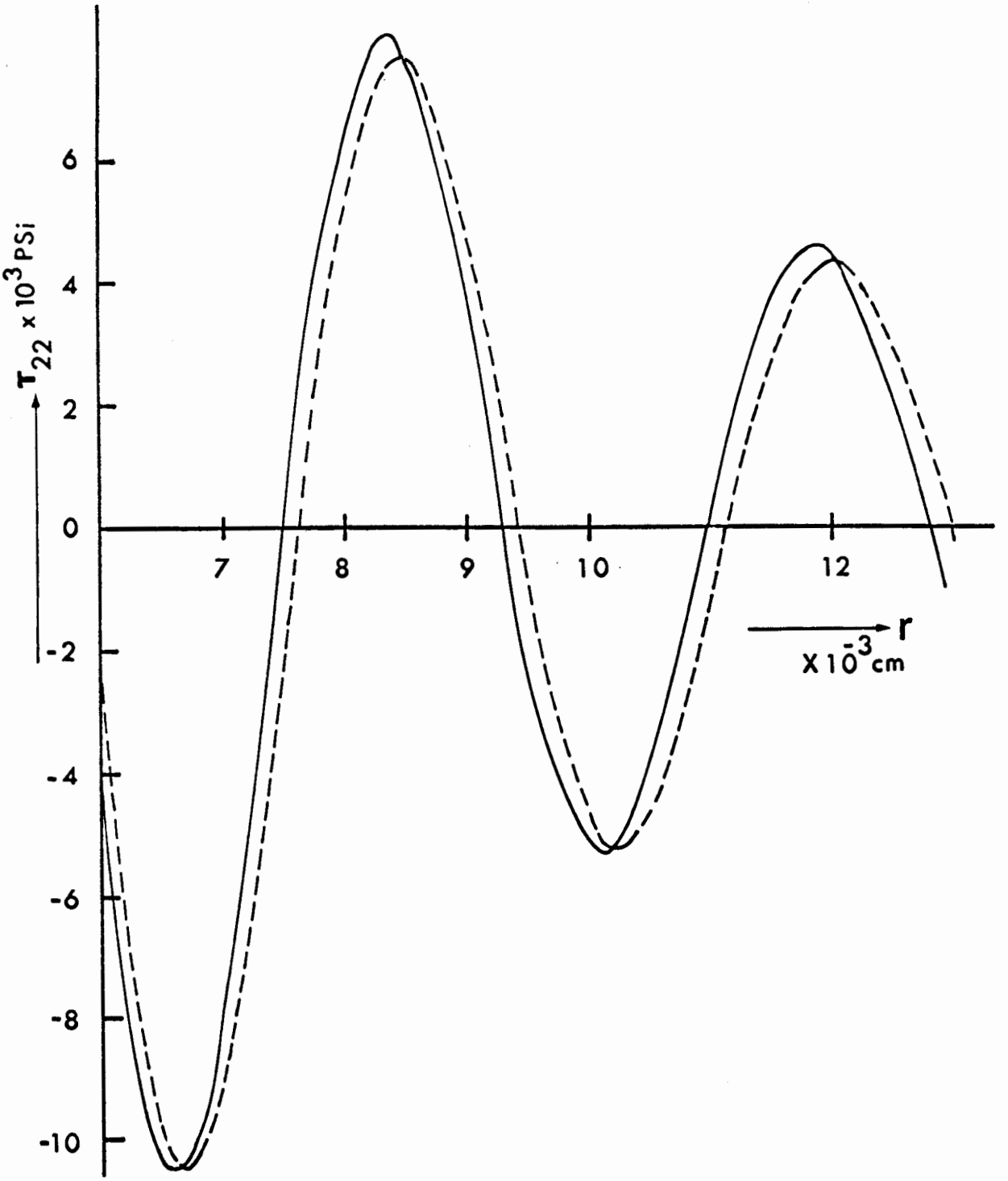

Fig. 2.3 Full Line $\omega = 7.85 \times 10^7$ sec^{-1}; k = 139, n = 65.

Dotted Line $\omega = 5.23 \times 10^7$ sec^{-1}; k = 93, n = 96.

amplitudes are almost equal but the positions of the peaks are slightly shifted. A similar shift occurs for the radial stresses too.

Stress fields were also calculated for different f-numbers of the focusing lens. The nature of the stresses remains the same but the amplitude of the stresses increases with decreasing f-value of the focusing lens. The peak amplitude of the hoop stresses at the edge of the Airy's disk increases as the square of f-value. Thus if the damage is caused by a pulse when focused by an f/10 lens, the stresses generated will not be sufficient to cause damage when the same pulse is focused by an f/15 lens. While using a lens of smaller f-value say f/5 the stresses generated will be four times higher thus driving the cracks much farther. This explains the severity of the damage when lenses of short focal lengths are used.

In the Appendix I the Griffith crack theory and Smekal's theory of voids were described. These theories assume the presence of a large number of small cracks on the surface or in the interior, rupture being primarily conditioned by the extension of a crack already existing and not by the formation of a new one. The spreading of the crack is accompanied by an increase in energy proportional to the increase of the surface, on the other hand internal surface increases the elastic deformability of the material thus leading to a lower free energy when the material is subject to a given external stresses.
It depends on the magnitudes and directions of crack and stresses

whether the total contribution is negative or positive. If an increase of the size of the crack leads to a diminution of the free energy, the system will become unstable and the crack will spread. From Figure 2.2, we see that the fracture is initiated by the tensile peaks of the hoop stresses which occur at distances of 0.03 mm. The cracks in the form of a spherical ring are forced open by the radial stresses. Typical speeds for the crack propagation in glass is 1/3 of the dilational velocity, so the next region will attain the fracture stress τ_{22} somewhat earlier in time than the time needed for the crack to reach this region. The cracks will propagate up to a certain distance until all the elastic energy is consumed in creating new fracture surfaces or if the crack meets a flaw or a step in the material. If at a flaw boundary the stress concentration is high enough it may lead to the branching of the cracks. Since the peak stresses near the focal point are much larger, these cracks will propagate further and merging of the consecutive crack disks occurs which gives the appearance of a pit or the pulverization of glass in that region.

The results of this analysis indicate that thermoelastically generated stresses, resulting from the optical absorption heating can explain most of features of the mechanical damage to glasses under irradiation by a high intensity Q-switched ruby laser. It must be noted that the absorption involved is not ordinary optical absorption but includes energy transferred by nonlinear effects. The value of the effective absorption coefficient ξ,

is obtained from the tensile stress fracture criterion and is found to be 50 cm^{-1} for the borosilicate glass and a Q-switched ruby laser pulse 30 n sec duration, with peak power density 3×10^9 watts/cm^2. For incident energy densities near threshold any nonlinear mechanism for the absorption must account for a minimum effective absorption coefficient of 50 cm^{-1} in the focal region.

CHAPTER IV

POSSIBLE MECHANISMS FOR ENERGY CONVERSION

The main interest in the study of the breakdown process of solids caused by intense laser radiation lies in the nature of the energy transfer mechanism. In the case of opaque materials the light absorption mechanism is well known. For transparent materials the mechanism of light absorption and the transformation of the absorbed energy into the breakdown energy is not at all clear. Several quite different mechanisms have been proposed. The three basic mechanisms for the mechanical breakdown of glasses by a Q-switched ruby laser pulse are:

(1) Electrostriction

(2) Accoustic wave generation by stimulated Brillouin scattering

(3) Multiphoton ionization and plasma formation.

We will discuss the first two mechanisms in this chapter and the details of the third mechanism are presented in the following chapters.

1. Electrostriction

Stresses caused by the direct action of light on dielectrics are due to:

(a) Direct light pressure

(b) Electrostrictive pressure due to the deformations by the electric stresses.

(a) Direct light pressure: This phenomenon is consistent with the concept of momentum of the electromagnetic waves. If an electromagnetic wave falls on an absorbing material and is not reflected, then its momentum is transmitted to the material in accordance with the conservation law for linear momentum. The rate of transfer of this momentum will be the force experienced by the body and is termed the light pressure. This rate of transfer in the case of totally absorbing body will be the momentum density of the radiation which is equal to the energy density divided by the speed of light. Thus the maximum light pressure will be $p = \frac{I}{c}$.

For an energy flux $I = 5 \times 10^9$ W/cm^2, we have

$$p = \frac{5 \times 10^{16} \text{erg/cm}^2 \text{ sec}}{3 \times 10^{10} \text{ cm/sec}}$$

$$= \frac{5}{3} \times 10^6 \text{ dynes/cm}^2$$

$$\simeq 2.5 \text{ psi}$$

Thus the maximum pressure due to the direct action of light in the case of transparent dielectric will not exceed 2.5 psi, which is very small.

(b) Electrostrictive pressure: This refers to the deformations produced by the electric stresses. Deformation of a dielectric in an electric field is determined partly by the Maxwell stresses and partly by the dependence of the dielectric constant upon the strain. In an electric field a dielectric tends to assume a configuration such as to reduce the total energy to a minimum. If, as is usually the case for glasses, the dielectric constant increases as the density increases, then Maxwell stresses and

the varying dielectric constant conspire to make the density increase when the field is applied. In some substances the dielectric constant decreases with increasing density. In such a case the state of minimum energy may be accompanied by a decrease in density.

These deformations, and the resulting electrostrictive pressure is proportional to the square of the electric field and is independent of its direction. The electrostrictive pressure can be evaluated by equating the work done on the dielectric to compress it to the change in the electrical energy[22].

Consider a condenser of volume V immersed in a compressible fluid. The change of electrical energy when the fluid constracts by an amount Δv is

$$\frac{E^2}{8\pi} V \left(\frac{d\epsilon}{dV}\right) \Delta V$$

where $d\epsilon$ is the change in the dielectric constant due to compression. Equating this energy to the amount of work done on the fluid $p_{el} \Delta V$

$$p_{el} \Delta V = \frac{E^2}{8\pi} V \left(\frac{d\epsilon}{dV}\right) \Delta V ,$$

Since

$$\frac{\Delta \rho}{\rho} = - \frac{\Delta V}{V} ,$$

where ρ is the mass density, we get

$$p_{el} = \frac{E^2}{8\pi} \cdot \rho \cdot \frac{d\epsilon}{d\rho} = \gamma \frac{E^2}{8\pi}$$

where $$\gamma = \rho \frac{d\epsilon}{d\rho}$$

is a constant having a value 0.6 to 1 for glasses.

Maximum electrostrictive pressure for an incident beam of intensity 5×10^9 W/cm^2 will be (for $\gamma = 1$) equal to:

$$p_{el} = \frac{5 \times 10^{16}}{c} \text{ erg/sec cm}^2$$

$$= 24 \text{ psi}$$

which is again very small when compared with the strength of glasses.

2. Stimulated Brillouin Scattering

In the normal Brillouin scattering an incident light beam is scattered by thermally excited acoustic waves. Scattered light is shifted in wavelength and the energy difference is taken up by the acoustic wave. A consideration of the energy and the phase vector conservation leads to the relations

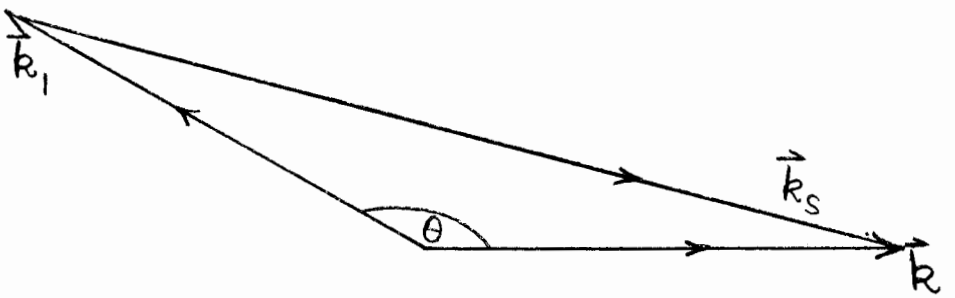

$$\omega = \omega_1 \pm \omega_s \quad (1)$$

$$\vec{k} = \vec{k}_1 \pm \vec{k}_s \quad (2)$$

where ω and k are the frequency and the phase vector of the incident light; ω_1, k_1 for the scattered light and ω_s, k_s for the acoustic wave. The well known Brillouin expression for the frequency shift is:

$$\omega - \omega_1 = \pm \omega_s \simeq \frac{2v_s}{c} n\omega \sin\frac{\theta}{2} \qquad (3)$$

where v_s, c/n are the acoustic and optical phase velocities in the medium, n is the index of refraction which will be essentially the same for incident and scattered light rays in isotropic media, and θ is their angular separation.

These relations imply that acoustic waves can either be generated or annihilated in the scattering process. When acoustic waves are generated, enhancement in light scattering can occur. With a weak exciting source enhancement is negligible but with a Q-switched laser pulse, the effect is profound. The process then leads to a marked regenerative behavior i.e. amplification of the scattered light. A brief sketch of the dynamics of the stimulated Brillouin scattering following Chiao et al[10] is presented below.

Coupling of the light waves with the sound waves is due to electrostriction, the compression or expansion of the material by the electric fields of the light wave. Consider two beams of light at slightly different frequencies in the medium

$$\vec{E}(\vec{r},t) = E_0 \cos(\vec{k}\cdot\vec{r} - \omega t + \phi) \qquad (4)$$

and

$$\vec{E}_1(\vec{r},t) = E_{10} \cos(\vec{k}_1\cdot\vec{r} - \omega_1 t + \phi_1) \qquad (5)$$

Let the sound wave be described by

$$P(\vec{r},t) = P_0 \cos(\vec{k}_s \cdot \vec{r} - \omega_s t + \phi_s) \tag{6}$$

The process of electrostriction causes a local compression δV, which in the presence of a local pressure P due to the sound wave does work by an amount

$$\delta W = P(\vec{r},t)\, \delta V(\vec{r},t) \tag{7}$$

The average power transferred to the sound wave per unit volume is:

$$\frac{du_s}{dt} = -\int \frac{d^3r}{V_0} \int_{-T/2}^{T/2} \frac{dt}{T}\, \vec{P}(\vec{r},t) \frac{\partial}{\partial t} V(\vec{r},t) \,. \tag{8}$$

where u_s is the energy density of the sound wave

$$\begin{aligned} -\frac{\delta V(\vec{r},t)}{V_0} &= \frac{1}{B}\, \delta P_{el}(\vec{r},t) \\ &= \frac{\gamma}{8\pi B}\, \delta\left[2\vec{E}(\vec{r},t) \cdot \vec{E}_1(\vec{r},t)\right] \end{aligned} \tag{9}$$

where B is the bulk modulus of the material. Considering only the resonant term equation (8) can be written as

$$\frac{du_s}{dt} = \frac{\gamma}{16\pi B}\, P_0 \left(\vec{E}_0 \cdot \vec{E}_1\right) \omega_s \tag{10}$$

where we have used $\vec{k} = \vec{k}_1 + \vec{k}_s$, $\omega = \omega_1 + \omega_s$ and $\Phi = \frac{\pi}{2} + \Phi_1 + \Phi_s$ The polarization produced by the sound wave gives rise to a dipole moment $\delta\vec{\mu}$, which in the presence of the local electric

field $\vec{E}_1$, leads to an energy transfer of:

$$\delta W = \vec{E}_1(\vec{r},t) \cdot \delta\vec{\mu}(\vec{r},t) \quad . \tag{11}$$

Thus the average power transferred to the scattered wave at the frequency ω_1 is

$$\frac{du_1}{dt} = \int \frac{d^3r}{V_0} \int_{-T/2}^{T/2} \frac{dt}{T} \vec{E}_1(\vec{r},t) \frac{\partial \vec{p}(\vec{r},t)}{\partial t} \quad . \tag{12}$$

where $\vec{p}(\vec{r},t)$, the induced polarization, is given by

$$\delta\vec{p}(\vec{r},t) = \frac{\Delta\epsilon}{4\pi} \vec{E}(\vec{r},t)$$

$$= \frac{\gamma}{4\pi B} \delta\left[P(\vec{r},t)\, \vec{E}(\vec{r},t)\right] .$$

Again considering the resonant terms only we get

$$\frac{du_1}{dt} = \frac{\gamma}{16\pi B} P_0 (\vec{E} \cdot \vec{E}_{10}) \omega_1 \tag{13}$$

If the plane of polarization of the $\vec{E}$ be perpendicular to the plane of the scattering or of $\vec{E}_1$, we can write:

$$\left(\frac{du_s}{dt}\right)_{gain} = \frac{\gamma \omega_s}{16\pi B} P_0 E_0 E_{10} \tag{14}$$

and

$$\left(\frac{du_1}{dt}\right)_{gain} = \frac{\gamma \omega_1}{16\pi B} P_0 E_0 E_{10}$$

The energy density of the sound wave u_s $\left(\equiv \frac{P_0^2}{2B}\right)$ will decrease due to the losses according to

$$\left(\frac{du_s}{dt}\right)_{loss} = -\frac{u_s}{\tau_s}$$

Similarly the energy density of the scattered wave u_1 ($\equiv \frac{\epsilon_1 E_0^2}{8\pi}$) will decrease as

$$\left(\frac{du_1}{dt}\right)_{loss} = -\frac{u_1}{\tau_1}$$

For the build up of the sound wave and the scattered wave gain must exceed the losses that is

$$\frac{\gamma \omega_s}{16\pi B} P_0 E_0 E_{10} \geq \frac{1}{\tau_s} \frac{P_0^2}{2B} \tag{15}$$

and

$$\frac{\gamma \omega_1}{16\pi B} P_0 E_0 E_{10} \geq \frac{1}{\tau_1} \frac{\epsilon_1 E_{10}^2}{8\pi} \tag{16}$$

Multiplying (15) and (16) we get the threshold condition for gain as

$$\frac{E_0^2}{8\pi} \geq \frac{1}{\omega_s \tau_s \omega_1 \tau_1} \cdot \frac{2B\epsilon_1}{\gamma^2} \tag{17}$$

Thus in order to have a catastrophic build up of sound and the Brillouin scattered wave, the incident intensity must be large enough to overcome the losses. For the case of fused quartz various constants are:(23)

$\gamma = 0.6$, $\tau_1 = 3 \times 10^{-9}$ sec, $\tau_s = 5 \times 10^{-9}$ sec.

$B = 10^{12}$ dynes/cm^2

$\omega_1 = 10^{15}$ sec^{-1}

$\omega_s = 10^{10}$ sec^{-1}

$$\frac{cE_o^2}{8\pi} \geq 100 \times \epsilon_1 \frac{MW}{Cm^2}$$

ϵ_1 is roughly 2.3, so the threshold energy density for the stimulated Brillouin scattering is 230 MW/cm^2. Kroll[24] in 1965 considered the problem of photoelastic instability in quartz and sapphire under illumination by an intense laser pulse. He solved the phenomenological equations, describing the photoelastic coupling between the electromagnetic and the elastic waves by a Lagrangian density

$$L_{int} = -\frac{1}{8\pi} p_{ijkl} D_i D_j \frac{\partial u_k}{\partial x_l}$$

where u_k refers to the displacements; D_i, the electric displacement vector and p_{ijkl} is the Pockel's elasto-optic constant. Results of his calculation show that the growth of a photoelastic excitation is governed primarily by an exponential factor of the form $(1.23\ W_\ell^{1/2}\ x^{1/2} - v_s \alpha t)$, where W_ℓ is the laser energy in Joules/cm^2, x is the interaction length, v_s is the sound velocity, α the attenuation at sound wavelengths, and t is the laser pulse duration. The backward instability is well developed when this exponent is of the order of ten or more. Kroll gives the following relation for the power carried by the elastic wave in terms of the power carried by the Stokes shifted wave,

$$P_s = \frac{\omega_s}{\omega} \cdot \frac{v_s t}{x} P_1$$

where ω_s is the elastic wave frequency, ω the incident laser frequency, P_s is the acoustic power and P_1 the power in the Stokes shifted wave. The build up of P_1, is limited by the failure of the linear approximation and in particular by the reaction back upon the incident laser power. Budin et al[25]

measured the Stokes light power for various incident laser energies for a silicate glass. From their data, for a focused ruby laser energy of 0.07 J or 210 J/cm^2 the Stokes shifted power is P_1 = 2000 W. Using Kroll's criterion for the instability we can calculate x:

$$1.25 W_l^{1/2} x^{1/2} - v_s \alpha t = 10.$$

Substituting all the values we get x = 0.30 cm. or the $P_s = 2 \times 10^{-4}$W. This yields an acoustic wave intensity of approximately 6 W/cm^2. Even if we assume that all this acoustic power is absorbed in the focal volume, the maximum value of the effective absorption due to this mechanism is $\xi = 0.1$, which is very much smaller than the minimum effective absorption needed for mechanical breakdown as deduced from energy considerations.

Ritus and Manenkov[26] investigated the threshold for stimulated Brillouin scattering and for the volume damage in glass, fused quartz and crystalline quartz. The results of their experiments are given below:

Material	Threshold for Stimulated Brillouin Scattering (P_{SBS})W/cm^2	Threshold for Volume damage $(P_{damage})_{w/cm^2}$
glass	10.9×10^9	8.9×10^9
Fused quartz	11.1×10^9	14.5×10^9
Crystalline quartz	8.9×10^9	31×10^9

ıe glass damage threshold found by us is lower, this discrepancy
attributed to the differences in the brand of glass. The
.ct that the damage is observed before the stimulated Brillouin
:attering threshold is reached indicates that stimulated Brillouin
:attering cannot be responsible for the damage in glass. If
ı the case of fused quartz and crystalline quartz, where P_{SBS}
lower than P_{damage}, and stimulated Brillouin scattering is
ıe damage mechanism then the damage threshold in crystalline
.artz should be lower than in fused quartz.

In addition we find that the material fracture is observed
ı crystals of CaF_2, MgO and NaCl when subjected to the focused
.ser radiation even when no stimulated Brillouin scattering is
:served. Clearly there must be some other mechanism of damage
:erating in these materials. Where stimulated Brillouin scatter-
:g does occur, the presence of this mechanism cannot be ignored.
:e details of this mechanism are given in the following chapters.

CHAPTER V

PHOTOCONDUCTIVITY IN GLASS INDUCED BY Q-SWITCHED RUBY LASER

istorical Sketch

Photoconductivity and photoelectric emission induced by ltraviolet light in soda glass, Pyrex and quartz were observed ı 1957 by Rohatgi[13]. Vul[27] and Culler and Rexford[28])served conductivity induced by gamma radiation in glasses. :ter the advent of high intensity lasers photoelectric ıission under laser excitation was observed in metals (see)r example Chang and Birdsall[29]), semiconductors and die- ;ctrics[30]. Laser induced photoconductivity in silicate .asses was first observed by Sharma and Rieckhoff[12]. The ıotoemission from metals and semiconductors can be explained r multiphoton ionization[31] or laser induced thermionic ıission[32]. It is shown here that photoconduction under :citation from a Q-switched ruby laser in silicate glasses .n be explained by multiphoton ionization.

All energetic electromagnetic radiations such as gamma .ys, X-rays, and ultraviolet light interact with both organic .d inorganic glasses. In each case color centers are produced[27,33]. .ese centers are qualitatively similar, but the number produced .d the lifetimes vary widely. Radiation is absorbed in different ys depending upon the energy of the quanta. X-rays and ultra- olet light are absorbed primarily by photoionization while gamma

ays may be absorbed by Compton scattering or pair production. n each case free electrons are produced with an energy which epends upon the incident photon energy. These free electrons e responsible for the production of the changes in the tructural units of the glasses involved. The changed units are dentified as the various types of color centers which are sponsible for the induced absorption bands in transparent asses. For example in alkali silicate glasses containing) mole % of alkali metal oxide, an absorption maximum occurs ; 3100Å when exposed to the X-rays or uv light, irrespective ' the alkali metal used. A second absorption maximum is also bserved whose position depends upon the particular alkali tal present in the glass. It is situated at 4150Å for lithium; ; 4500Å for sodium, at 4750Å for potassium, at 4850Å for rubidium id at 4900Å for cesium. The exact position of the absorption ak at 3100Å depends upon the alkali oxide concentration and ifts to lower wavelength with decreasing alkali metal con- ntration, while the absorption peaks around 4500Å do not pend upon concentration. The absorption peak at 3100Å is tributable to nonbridging oxygens which have lost an electron, ile the peak around 4500Å is due to the interstitial alkali tal cation which has captured an electron, and thus its position ries depending upon the alkali metal used. These absorption nds are bleached by heating or by shining light on them.

The energy of photons produced in ruby lasers is 1.78 ev. is is far below the energy needed to produce a free electron

ı glasses of this kind. However, at high photon flux densities 10^{27} photons cm^{-2} - sec^{-1}, three or four of the ruby laser ıotons can be absorbed simultaneously.(14) They then produce ıe same effect which is observed under illumination by X-rays ; ultraviolet light, although the efficiency of this process ; very small by comparison. We present here the results of ‹periments in which the contribution of the electrons produced / such a process to the electrical conductivity of the glasses ıder study is observed.

‹perimental Arrangement

Figure 5.1 shows the basic experimental set up. The laser ;ed is a Raytheon LH5 laser head with a high quality 60° ruby ‹ystal, six inches long and 3/8 inch in diameter. Vanadium ıthalocynanine in benzene was used as a passive Q-switch and a)° prism as an end reflector. The laser cavity was cooled by ry, cold nitrogen to a temperature of -5°C. This temperature as held constant to within 1°C in order to obtain reproducible aser pulses. This was achieved by attaching a disc thermistor JB31J) to the ruby crystal holder and using this in one arm of ıe Wheat Stone bridge circuit shown in figure 5.2. The bridge as balanced at -5°C by adjusting the 1K potentiometer. Any luctuations in the cavity temperature will vary the resistance f the thermistor and will produce corresponding changes in oltage at the points A and B. These voltage changes are fed

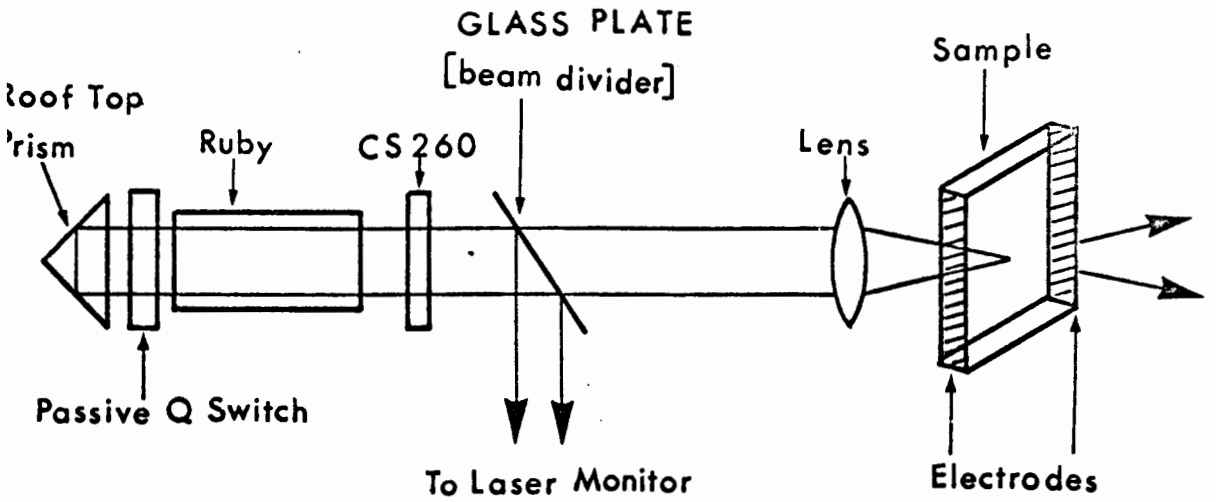
GLASS PLATE
[beam divider]
Sample
Roof Top
Prism
Ruby
CS 260
Lens
Passive Q Switch
To Laser Monitor
Electrodes

Fig. 5.1

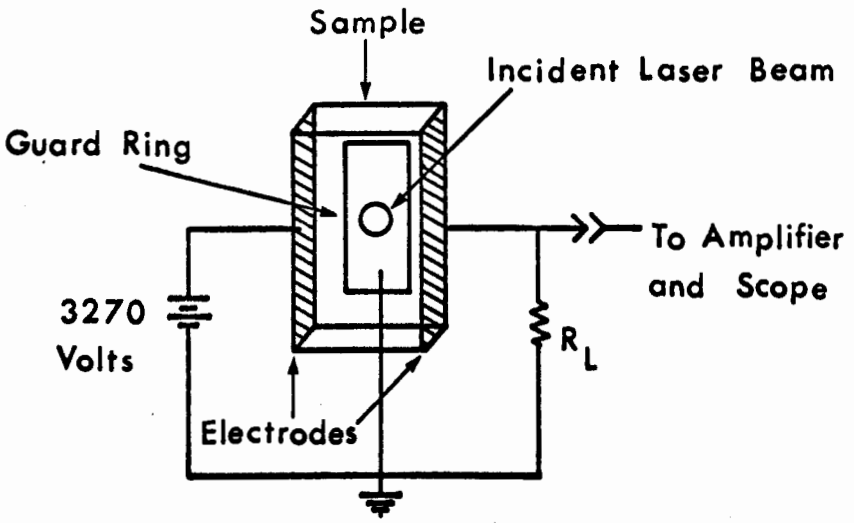
Sample
Incident Laser Beam
Guard Ring
To Amplifier
and Scope
3270
Volts
R_L
Electrodes

Fig. 5.4

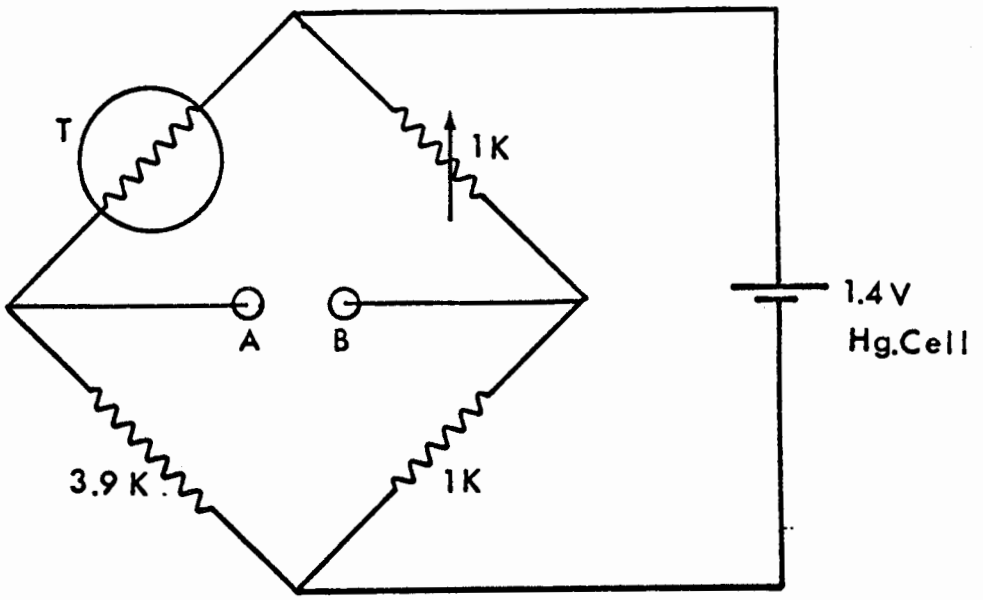
T
1K
A
B
1.4 V
Hg.Cell
3.9 K
1K

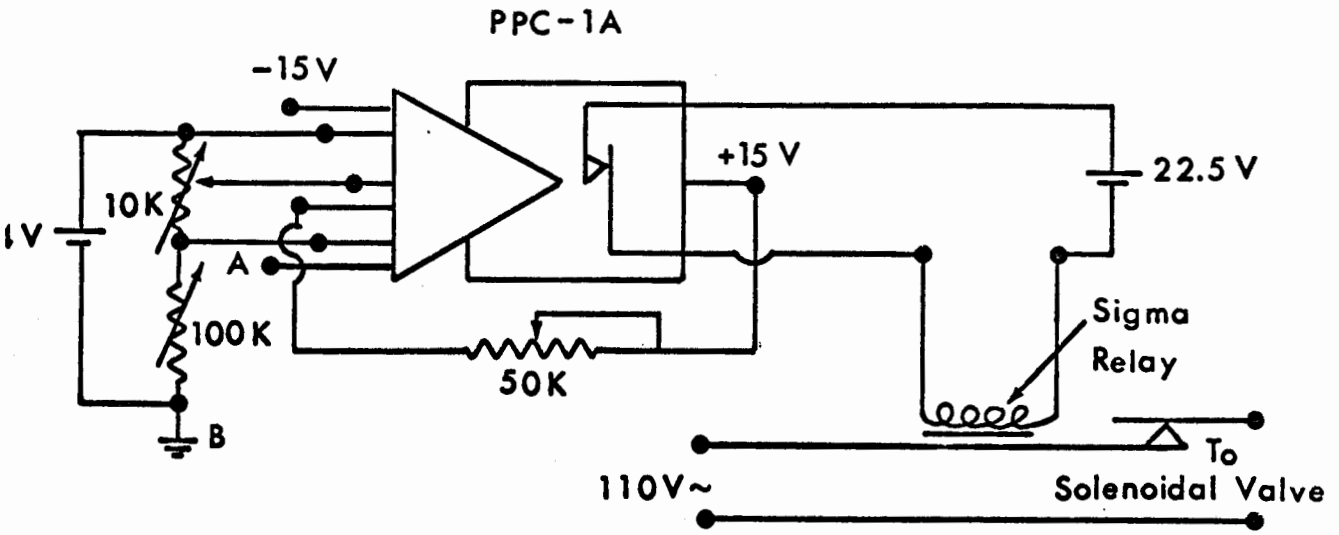
PPC-1A
-15 V
10K
A
100K
B
50K
+15 V
22.5 V
Sigma
Relay
To
Solenoidal Valve
110V~

Fig. 5.3

nto a picopower comparator relay (DDC type PPC-1A) as shown n figure 5.3, which provides the contact closure when the nput voltage is 1/2 millivolt greater than the reference oltage. This relay then actuates a solenoidal valve thus onnecting or cutting off the flow of cooled dry nitrogen o the laser cavity. A small flow of dry nitrogen is main-ained through the laser cavity to prevent the silver from etting tarnished. The laser output was monitored using a icroscope slide as beam splitter. Four per cent of the ncident pulse energy was reflected and attenuated by a olution of Nickel Sulfate in water and neutral density ilters before hitting the photocathode of an RCA 925 photo-iode. The output of the laser consisted of pulses of 20 nano-econd half width and a peak power of 2-3 megawatts. The light rom the Q-switched ruby laser was partially focused in the ample by a 10 cm focal length lens. The diameter of the beam ncident on the sample was about 1 mm. A corning glass filter -60 was used to prevent short wavelength light from the laser mp from reaching the sample. The samples used were rectangular ieces of soda glass, fused quartz and quartz crystal, with nickness 0.15 cm to 0.20 cm. The spacing between the elec-odes was 0.7 cm. To make electrical contacts to the glass ne samples were cleaned with hydrofluoric acid and gold wire eads were stuck to the sides with the aid of high purity ndium. Silver was then evaporated on the sides to give a niform field across the sample as shown in the figure 5.4. tteries were used to apply the d.c. voltage across the sample.

o eliminate conduction along the surface of the samples, a rounded electrode surrounding the area of irradiation was vaporated onto the surface. The applied field inside the ample will in principle be altered by the presence of this uard ring as well as the fraction of the charges reaching the lectrodes. In arriving at our final results we can neglect ne presence of the guard ring for the following two reasons: 1) the detailed geometry of the sample decreased the influence f the guard ring inside the sample; (2) we obtain identical esults when using samples without guard rings. In other words uard rings merely provide assurance that the surface effects are ot important. Polarization effects due to the migration of the obile Na^+ were neglected[34] since all experiments were done n times short compared with the time needed to produce such olarizations. Our experiments are performed at room temperature nd in light. Any electrons trapped as color centers will be leached in the time interval of 3-5 minutes between successive aser shots.

For studies of the intensity dependence of the effects, orning glass filters were used as attenuators in the laser eam. While studying the intensity dependence of the photo- onductivity induced by the laser it was noticed that the onductivity gave rise to a signal many orders of magnitude higher han usual if the intensity was high enough to cause mechanical amage. This provided an easy criterion to assure that the aser power was always kept below the level at which the dielectric reakdown effects such as sparking etc. occurred.

:perimental Results

Figure 5.5 shows a typical signal obtained. The upper
'ace shows the voltage across R_L resulting from the photo-
ırrent. The collected charge Q_c is obtained from the area under
ıe lower curve. The life time of the charge carriers τ_r is
)und from the shape of the lower curve. Knowing Q_c and τ_r
ıe number of electrons n_0 generated by the laser pulse can be
)tained. In figure 5.5, the sample is a quartz crystal, the
.ser power is 2.9 MW corresponding to an incident flux on the
.mple of 1.28×10^{27} photon $cm^{-2}\ -s^{-1}$, and the total charge
)llected Q_c is 6.38×10^{-13} Coulomb or 4×10^{7} electrons. A
.ot of the total charge collected Q_c (Coulombs) against the
ıcident photon flux S (photons / $cm^2 s$) is given in figure 5.6,
)r the case of soda glass, fused quartz and quartz crystal.
.e straight lines are obtained by a least squares fit of the
.ta. This gives a relation $Q \propto S^m$ and the slopes of the lines
.ve the values for m, which are

glass	fused quartz	quartz x-tal
$m = 3.4 \pm 0.8$	3.8 ± 0.4	3.6 ± 0.6

e shape of the current pulse was the same in all three cases.
e time delay between the peak of the laser pulse and the peak
the photocurrent is dependent on the time constant of the
paratus τ_a.

To obtain an expression for the photocurrent I(t), we
nsider a sample with a distance ℓ between the electrodes and

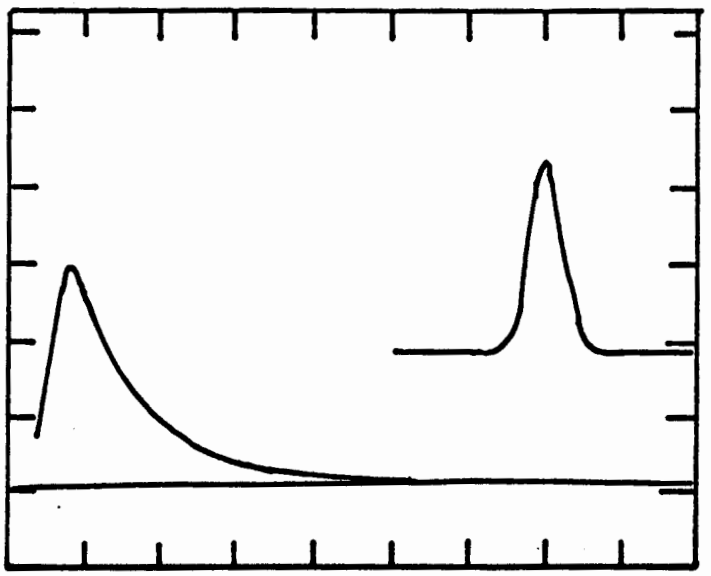

Fig. 5.5

Typical Signal. Upper trace, Q spoiled laser pulse t = 40 ns/div. Lower trace, amplified signal voltage across R_L(= 1MΩ) t = 0.1 ms/div., and sensitivity 0.1 V/div.

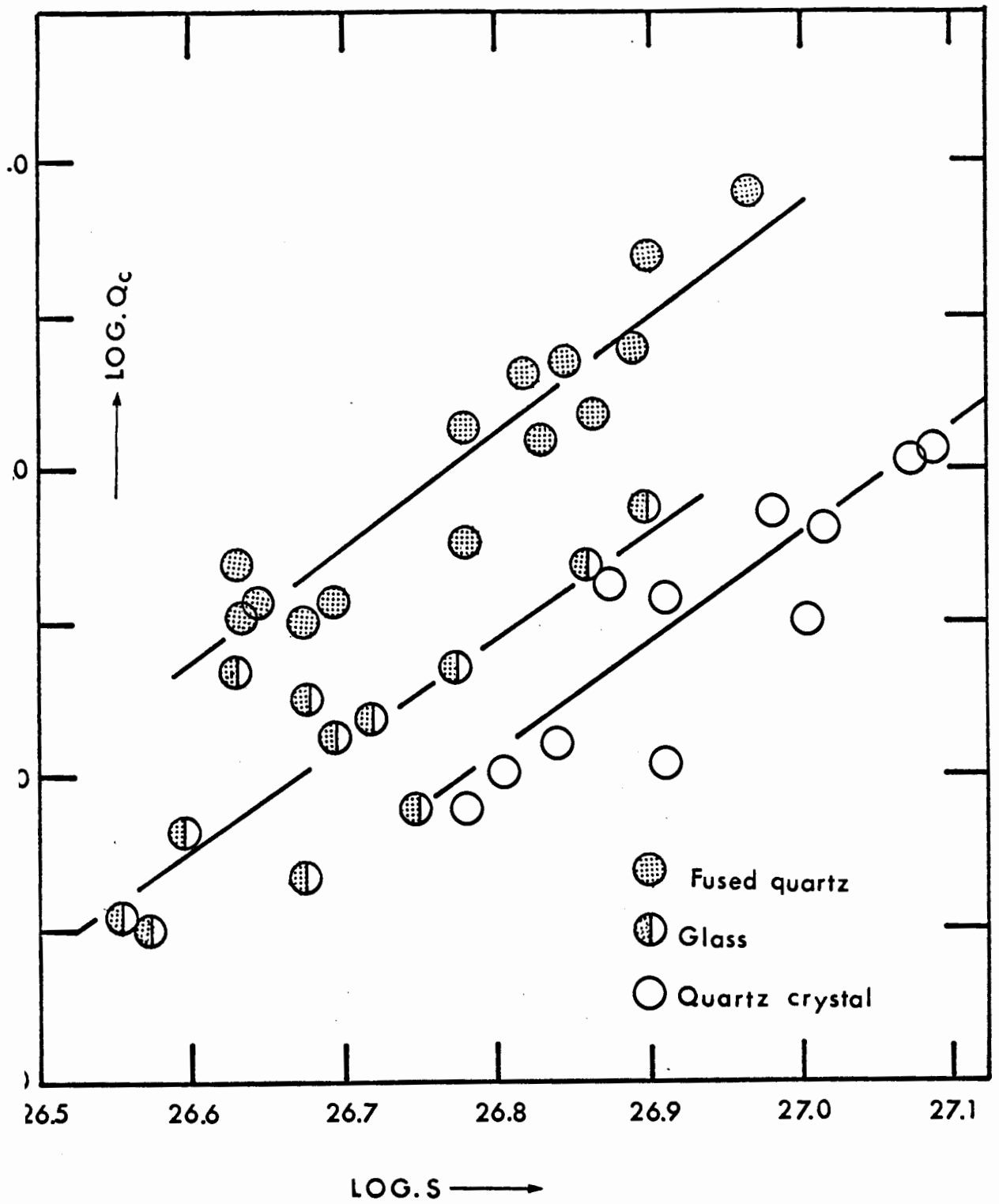
LOG. Qc
LOG. S
26.5
26.6
26.7
26.8
26.9
27.0
27.1
Fused quartz
Glass
Quartz crystal

Fig. 5.6

luminated at the center. The illumination produces n_0 ectrons in a time of 20 ns. Let μ be the mobility of these ectrons and τ_r their lifetime in the conduction band. We sume that the recombination process is linear and can be aracterized by a single lifetime. This is justified in ew of the very large concentration of recombination centers ch as metallic ions, oxygen vacancies, etc. Under the effect an applied electric field E, these electrons drift towards e anode. They will also diffuse. We now derive an expression r the current density using phenomenological parameters:

Consider the one dimensional motion of electrons. The rrent density taking into account drift and diffusion of rriers is

$$j(t) = eD\frac{\partial n(t)}{\partial x} + e\mu E n(t) \qquad (1)$$

ere D is the diffusion coefficient, μ is the mobility of ectrons, n(t) the number of electrons at time t after the lse, E the effective field and e the electronic charge.

$$E = E_0 + E_1 \qquad (2)$$

re E_0 is the applied field E_1 is the field due to the electrons ven by

$$\frac{\partial E_1}{\partial x} = \frac{4\pi e}{\epsilon} n \qquad (3)$$

ere ϵ is the dielectric constant. From the continuity uation

$$\frac{\partial n}{\partial t} = -\frac{n}{\tau_r} + \frac{1}{e}\frac{\partial j}{\partial x} \tag{4}$$

ere τ_r is the lifetime of the electrons. Substituting for in (4)

$$\frac{\partial n}{\partial t} = -\frac{n}{\tau_r} + D\frac{\partial^2 n}{\partial x^2} + \mu E\frac{\partial n}{\partial x} + \mu n\frac{\partial E_1}{\partial x} \tag{5}$$

r convenience we assume a Gaussian distribution in x for e electrons. The half width of the Gaussian is assumed to 1/4 times the focal diameter of the beam because of the ur photon nature of electron generation

$$n(x) = \frac{n_o}{\sqrt{2\pi\sigma}} \exp.\left(-x^2/2\sigma^2\right) \tag{6}$$

ere σ is the half width. Then from (6)

$$\frac{\partial n}{\partial x} = -\frac{x}{\sigma^2} n \tag{7}$$

d

$$\frac{\partial^2 n}{\partial x^2} = \left(-\frac{1}{\sigma^2} + \frac{x^2}{\sigma^4}\right) n$$

bstituting for $\frac{\partial n}{\partial x}$, $\frac{\partial^2 n}{\partial x^2}$, $\frac{\partial E_1}{\partial x}$ and $D = \frac{\mu kT}{e}$, we obtain

$$\begin{aligned}\frac{\partial n}{\partial t} &= -\frac{n}{\tau_r} + \frac{\mu kT}{e}\left(\frac{x^2}{\sigma^4} - \frac{1}{\sigma^2}\right) n \\ &\quad - \frac{\mu E x}{\sigma^2} + \mu n \frac{4\pi e}{\epsilon} n. \\ &= -\frac{n}{\tau_r} + \mu n E\left[\frac{kT}{eE}\left(\frac{x^2}{\sigma^4} - \frac{1}{\sigma^2}\right)\right. \\ &\quad \left. - \frac{x}{\sigma^2} + \frac{4\pi n e}{\epsilon E}\right].\end{aligned} \tag{8}$$

e relative magnitude of the various terms in the square brackets

$$\frac{4\pi ne}{\epsilon} = 8 \times 10^{-8}\ cm^{-1}.$$

$$\sigma = \frac{1}{4}d = 0.025\ cm\ ;\ \sigma^{-2} = 6.25 \times 10^{-4}\ cm^{2}.$$

$$\frac{kT}{eE} = 1.7 \times 10^{-5}\ cm.$$

$$\mu = 10^{-5}\ cm^{2}/Volt\ sec.$$

Let $x = 10^{-5}\ cm$, then

$$\frac{\partial n}{\partial t} = -\frac{n}{\tau_2} + n\mu E\left[1.7\times10^{-5}(2.25\times10^{-4} - 1.5\times10^{3}) - 1.5\times10^{-2} + 8\times10^{-8}\right].$$

glecting the last term in the square brackets and integrating

) we get

$$n = n_0 \exp\left[-\frac{t}{\tau_2} + \mu E t\left\{\frac{kT}{eE}\left(\frac{x^2}{\sigma^4} - \frac{1}{\sigma^2}\right) - \frac{x}{\sigma^2}\right\}\right] \qquad (9)$$

bstituting for n in (1)

$$i(t) = \mu E n_0 e.\ e^{-t/\tau_2}\left[1 - \frac{\mu kT}{eE}.\frac{x}{\sigma^2}\right] \times \exp.\left[\mu E t\left(\frac{x^2}{\sigma^4} - \frac{1}{\sigma^2}\right) - \frac{x}{\sigma^2}\right].$$

$$= \mu E n_0 e.\ e^{-t/\tau_2}(1 - 2.5\times10^{-12})\left[1 + t\left\{\frac{\mu kT}{e} \times \left(\frac{x^2}{\sigma^4} - \frac{1}{\sigma^2}\right) - \frac{\mu E x}{\sigma^2}\right\}\right]$$

$$= \mu E n_0 e.\ e^{-t/\tau_2}\left[1 + t\left\{8.6\times10^{-7}(-1.5\times10^{3}) - 7.5\times10^{-4}\right\}\right]$$

$$= \mu E n_0 e.\ e^{-t/\tau_2}\left[1 - 2\times10^{-3}t\right].$$

ow t can have a maximum value of $10\tau_r$ which is $\sim 10^{-4}$ sec, so
ie current density to this approximation becomes

$$j(t) = \mu E e n_0 \cdot e^{-t/\tau_r} = \mu E e n(t) \qquad (11)$$

his is the required expression for the current density. The
harge collected by the electrodes will be e if an electron
ravels right across the sample,[35] but if the electron travels
distance x only, the charge measured will be $\frac{ex}{\ell}$. The distance
ravelled in unit time is $x = \mu E$. Thus the charge delivered to
.e electrodes in unit time is

$$I(t) = n_0 e\left(\frac{\mu E}{\ell}\right) e^{-t/\tau_r} = I_0 e^{-t/\tau_r} . \qquad (12)$$

ie measuring circuit and its equivalent circuit are shown in
gure 5.7. Here C_s is the sample capacitance, R(t) is its
sistance, R_L is the load resistance and C is the distributed
pacity. Current flowing through R_L produces the signal voltage.
ie time dependence of this voltage will be the time dependence
I(t), (given by (12)) modified by the response of the R_LC
rcuit. If the impedance of the (R_LC) part is very small as
mpared with that of the sample, the magnitude of the current
ll be controlled by the sample impedance. The circuit 5.7(a)
duces to an equivalent circuit shown in figure 5.7(b). This
ves the voltage drop across R_L

$$V(t) = \frac{\mu E n_0 e}{\ell} \cdot \frac{\tau_a \tau_r}{C(\tau_r - \tau_a)} \left(e^{-t/\tau_r} - e^{-t/\tau_a}\right) . \qquad (13)$$

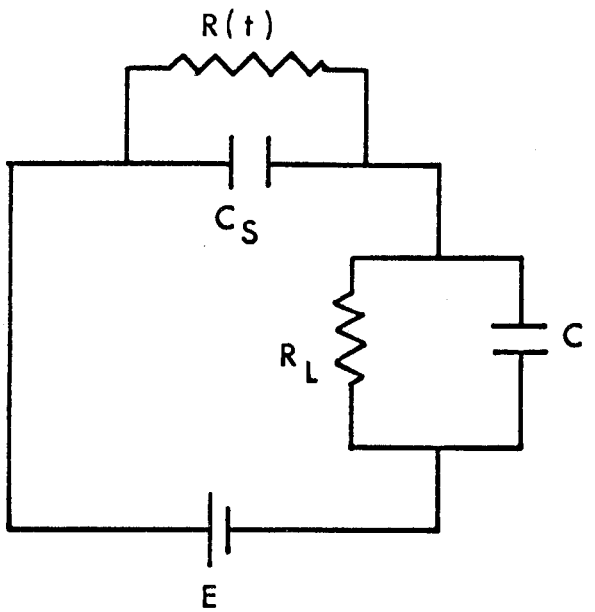

(a)

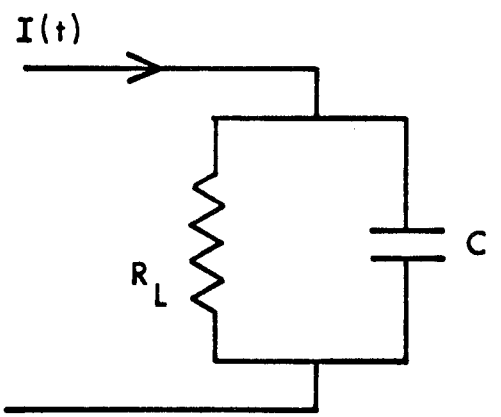

(b)

Fig. 5.7

ere $\tau_a = R_L C$, the time constant of the apparatus. The total
arge collected will be

$$\frac{1}{R_L}\int_0^\infty V(t)\,dt = \frac{\mu E n_o e}{\ell}\cdot\frac{\tau_a\tau_r}{R_L C(\tau_r-\tau_a)}\int_0^\infty (e^{-t/\tau_r} - e^{-t/\tau_a})\,dt.$$

$$Q_c = \frac{\mu E}{\ell}\,\tau_r \cdot n_o e$$

$$n_o = \frac{Q_c}{e}\cdot\frac{\ell}{\mu E \tau_r} \qquad (14)$$

obtain τ_r from the shape of the signal we consider

$$\frac{V(t)}{V(max)} = \frac{e^{-t/\tau_a} - e^{-t/\tau\cdot\tau_a}}{e^{-\frac{\tau\ln\tau}{\tau-1}} - e^{-\frac{\ln\tau}{\tau-1}}}$$

ere

$$\tau = \tau_r/\tau_a$$

e value of τ is found by the best fit to the experimental
rve. Since we know the value of τ_a, τ_r is found to be of the
der of 10^{-5}s. The values of τ_r do not differ much in the
ree cases investigated. From the position of the maximum of
t) on the trace the estimate of τ_r can be justified. If
$\leq 0.1\ \tau_a$ the maximum would occur essentially with a time
lay of $\leq 0.2\ \tau_a$. For $\tau_r \geq 0.9\ \tau_a$ the maximum would not be
en on the time scale used on the photographs. Since the
ximum does in fact occur with excellent reproducibility
tween these extremes we obtain the above mentioned value
τ_r from a best fit of our data. For comparison of the

elative magnitude of the effect in various materials, we calculate ne proportionality constant α in the relation $n_0 = \alpha S^m$ for an ncident photon flux of 6.3×10^{26} photons/(cm^2 - sec) and assum- ng m = 4 for all the cases we find:

$$\alpha = (1.20 \pm 0.03) \times 10^{-95} \quad \text{Fused quartz}$$

$$= (1.69 \pm 0.01) \times 10^{-96} \quad \text{Glass} \qquad (15)$$

$$= (1.08 \pm 0.05) \times 10^{-96} \quad \text{Quartz Crystal}$$

iscussion

To interpret the results it is appropriate to refer to ir understanding of the structure of silicate glasses (Appendix). In the nonirradiated state quartz crystal, fused quartz id glass do not absorb in the visible region. The absorption pectra shows a hump around 2350Å is fused quartz and a fundamental psorption around 1800Å and below in fused quartz and quartz rystal. Kats and Stevels[33] also found such a hump in soda lass. In the case of glass absorption starts at 3100Å - 2600Å epending upon the composition (figure 5.8). The absorption 2300Å results from the transition of an electron from a non- ridging oxygen to the conduction band and the fundamental psorption at 1800Å in fused quartz and quartz crystal results n the liberation of an electron from the bridging oxygens[33]. or quartz crystal with a more perfect lattice than fused quartz ne absorption at 2300Å is hidden under the tail of the fundamental

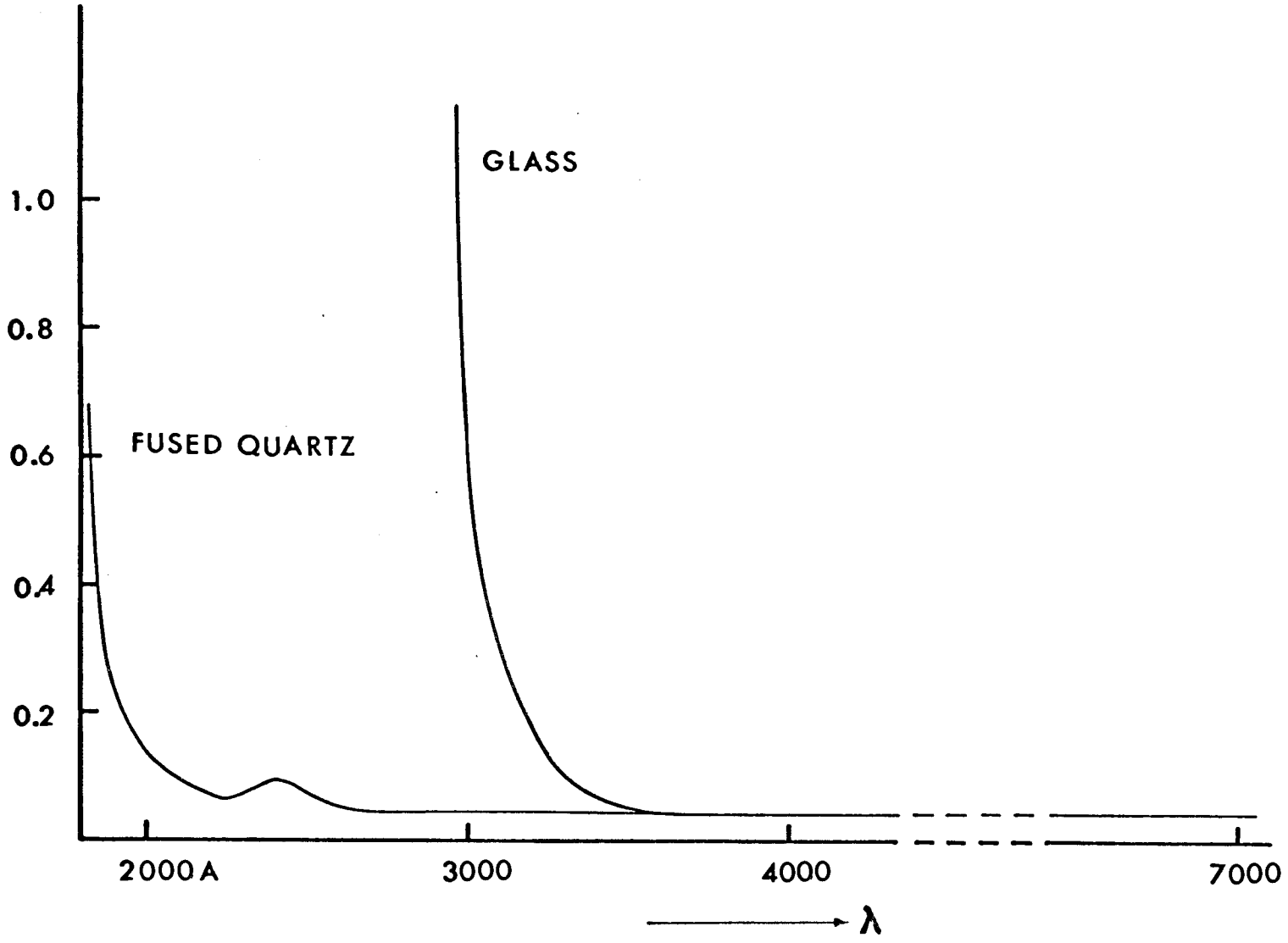

Fig. 5.8

Spectral Transmission curves for Fused Quartz and Glass

sorption, indicating that the number of nonbridging oxygens
crystals is down by approximately an order of magnitude. The
nbridging oxygens in soda glass will emit an electron under
citation by electromagnetic radiation, i.e. an electron is
berated by the reaction

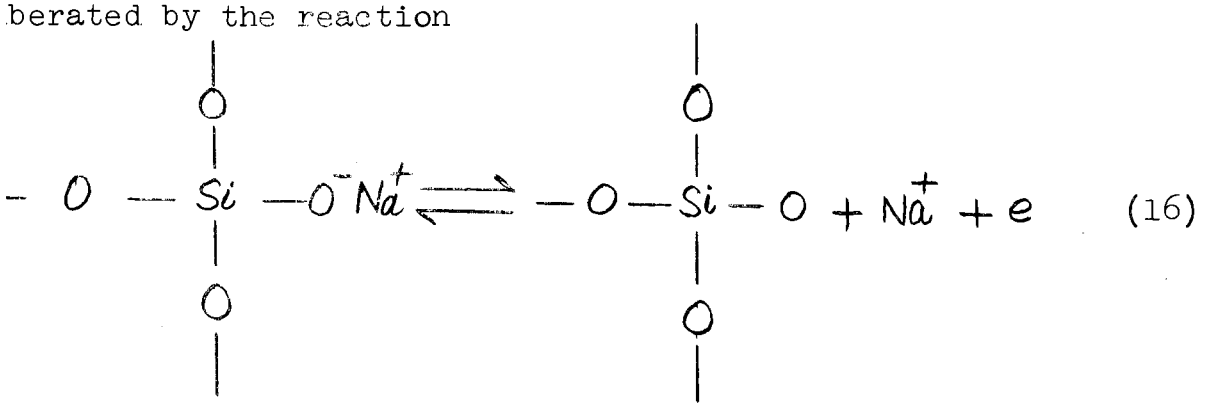

(16)

ter the electron has been ejected then Na+ becomes mobile
d the d-c conductivity will be increased and the more
ergetic electrons may be observed as photoelectric emission
om glass. Because the ionization energy of Sodium atoms is
1 ev and thus near the energy of photons λ = 2300Å, Rohatgi[13]
tributed this photoelectric emission to the ionization of
dium atoms, assuming the presence of 10^{13} sodium atoms per
^{2} in a 10Å thick surface layer of glass. However, the
dium in glass is, in fact, present as a charge compensating
n. It is clearly shown by the x-ray diffraction experiments
at the bonding between the oxygen ions and sodium ions is
ghly ionic. These sodium ions could not be ionized again by
e ultraviolet light used in these experiments. The increase
d-c conductivity observed by Rohatgi must be a result of the
ission of electrons from nonbridging oxygen ions, whereafter

ıe sodium ions, no longer required as charge compensators
:come mobile.

The relative magnitude of photoconductivity induced by
ıe laser beam also suggest that the electron is not liberated
r the ionization of sodium in glass. We observed a yield from
ısed quartz (< 1% Na or other alkaline metals) almost an order
' magnitude higher than that from soda glass (13% Na). The
.eld in quartz crystal was smaller than that in either glass
· fused quartz. This is not surprising in view of the scarcity
' nonbridging oxygens in a more perfect lattice as evidenced
r the absence of the absorption peak around 2300Å. We interpret
ıe observed photoconductivity under laser excitation as multi-
ıoton excitation of an electron into the conduction band. The
.ngle photon energies needed to induce such a transition from
ıe nonbridging oxygens is 5.36 ev and from bridging oxygens
.86 ev. The number of ruby photons of energy 1.78 ev needed
› induce these transitions will be four. Thus in both cases
ıe electron excitation probability should be proportional to
. That in fact a smaller figure is observed experimentally
ın easily be understood, considering the width of the absorption
:aks. There can be no doubt that there exists a considerable
ımber of oxygens located in surroundings such that the energy
›r liberation of an electron is reduced to below 5.34 ev, in
ıich case three ruby photons will be sufficient to produce
ıotoconductivity, since the tail of the absorption in quartz

tends well below 5.34 ev. In glass there is a very strong sorption below 5.34 ev, but the effect observed is smaller an that in fused quartz and still shows the same power pendence on the intensity of the incident light. This is cause the strong absorption in glasses at longer wavelengths due to the variable valency metallic ions (such as Fe^{++}) our samples which also gives a greenish tinge to the glass. is is not a contradiction of our mechanism if one interprets e strong absorption below 5.34 ev in glass as arising essentially om excited states of the impurities present, which do not ntribute to the photoconductivity by either single or multi- oton processes. Rohatgi[13] did not observe photoconductivity this region of the spectrum in glasses.

To obtain an estimate for the cross section σ for a multi- oton absorption process liberating an electron from the oxygen let N be equal to the density of the ionizable atoms (Bridging non bridging oxygens) which is ~ $10^{22}/cm^3$. V is the focal lume. Then the number of electrons n generated by the photon ux of S photons/cm^2 sec in the time Δt is

$$n = NV\sigma S\Delta t \tag{17}$$

$$\sigma(S) = \frac{n}{NVS\Delta t} \tag{18}$$

e values obtained for σ in the three samples, with a photon ux of 6.3 x 10^{26} photons/cm^3 are

Glass	Fused Quartz	Quartz Crystal
$3 \times 10^{-30} cm^2$	$10^{-29} cm^2$	$10^{-30} cm^2$

n fact we expect σ to be roughly the same for these cases and
ne number of nonbridging oxygens to be the variable quantity.

ultiphoton ionization

From general considerations, the behaviour of an atom in strong radiation field, whose energy of interaction with the tomic electrons approaches the energy of interaction of lectrons with nucleus, will differ qualitatively from the usual ehaviour predicted by the perturbation theory of quantum ransitions. For these field intensities the condition for esonance transitions derived in the first approximation of erturbation theory is violated. In this case, from the point f view of perturbation theory, many-photon processes become ominant and take place with a probability comparable to that f single photon processes at ordinary light levels. If the nteraction time of the atom with the radiation field is sufficiently ong, then the most probable process is the ionization of the tom and not its excitation to a bound electron state, even nough the quantum of the field $\hbar\omega$ is many times smaller than ne ionization potential. An example of such a process is the uch studied ionization of the hydrogen atoms in a constant lectric field.[36] The potential energy of the electron in he external field when added to its potential energy within

ıe atom, has an effect such that the region of possible
ɔtion for the electron (whose total energy E is negative)
ıcludes, besides the region inside the atom, the region of
ırge distances from the nucleus in the direction of the anode.
ıese two regionsare separated by a potential barrier, whose
idth diminishes as the field increases. Quantum mechanically
ɔeaking, there is a finite probability that a particle will
ɜnetrate the potential barrier, i.e. the electron will emerge
ɔom the region within the atom and this is simply the ioniza-
ion of the atom.

ınnelling Theory

Keldysh[37] considered this tunnelling of the electrons
ı the field of a strong electromagnetic wave. He calculated
ıe transition probability from the ground state to the
ɔntinuous spectrum viz:

$$W_0 = \frac{1}{\hbar^2} \int_{\lim T\to\infty} \frac{d^3p}{(2\pi\hbar)^3} \left| \int_0^T dt \cos\omega t \; V_0\left(\vec{p} + \frac{e\vec{F}}{\omega}\sin\omega t\right) \right.$$
$$\left. \times \exp\left[\frac{i}{\hbar}\int_0^t I_0 + \frac{1}{2m}\left(\vec{p} + \frac{e\vec{F}}{\omega}\sin\omega\tau\right)^2 d\tau\right] \right|^2 \qquad (20)$$

ıere

$$V_0(\vec{p}) = \int e^{-i\vec{p}.\vec{r}} \; e\vec{F}.\vec{r} \; . \; e^{-r/a_0} \frac{d^3r}{\sqrt{\pi a_0^3}} \; . \qquad (21)$$

ɜ the matrix element between the initial ground state $\frac{1}{\sqrt{\pi a_0^3}} e^{-r/a_0}$

ıd the final state

$$\psi(\vec{r},t) = \exp.\frac{i}{\hbar}\left[(\vec{p}+\frac{e\vec{F}}{\omega}\sin\omega t).\vec{r} - \int_0^t (\vec{p}+\frac{e\vec{F}}{\omega}\sin\omega\tau)^2 d\tau\right]$$

ıe main difference between this procedure and the usual
:rturbation theory is the fact that here we calculate the
'obability of transition not to a stationary final state but
› a state $\Psi(r,t)$ that already takes account of the acceleration
' free electrons in the electric field.

Solving this in the limit (tunnelling frequency is much
ıaller than laser frequency)

$$\gamma\left(\equiv \frac{\omega\sqrt{2mI_0}}{eF}\right) \gg 1$$

: get the probability of ionization by the absorption of
:veral photons:

$$W_0 = A\omega\left(\frac{I_0}{\hbar\omega}\right)^{3/2}\exp\left\{2\left\langle\frac{\tilde{I}_0}{\hbar\omega}+1\right\rangle - \frac{\tilde{I}_0}{\hbar\omega}\left(1+\frac{e^2F^2}{2m\omega^2I_0}\right)\right\}\times\left(\frac{e^2F^2}{8m\omega^2I_0}\right)^{\left(\frac{\tilde{I}_0}{\hbar\omega}+1\right)} \times \Phi\left[\left(2\left\langle\frac{\tilde{I}_0}{\hbar\omega}+1\right\rangle - 2\frac{\tilde{I}_0}{\hbar\omega}\right)^{1/2}\right]. \qquad (22)$$

ıere $\tilde{I}_0 = I_0\left(1+\frac{e^2F^2}{2m\omega^2I_0}\right)$ (I_0 being the ionization potential)
·electronic charge, m its mass, ω the ruby laser frequency
ıd F is the effective field in the pulse. A is a constant of
ıe order of unity and the angular brackets means that the quantity
ıclosed is approximated to the nearest integer. The function
(z) is Dawson's probability integral defined as

$$\Phi(z) = \int_0^z e^{(y^2 - z^2)}\, dy \,.$$

ing equation (22) we can estimate the cross section for
ltiphoton ionization taking a value of 4 for $\langle \frac{I_0}{\hbar\omega} + 1 \rangle$.
e quantity

$$\frac{e^2 F^2}{2m\omega^2 I_0}$$

n be written as

$$\frac{2\pi e^2}{mc\omega^2 I_0} \times \frac{10^{-24}}{1.1} \times S$$

ere S is the photon flux. For an incident photon flux of
3×10^{26} photons/cm^2 sec. we get for the ionization probability
$= 1.5 \times 10^{-6}$ sec. or the cross section for ionization per
it incident flux we get

$$\sigma = \frac{W_0}{S} = 2.4 \times 10^{-33} \text{ cm}^2.$$

mparing this with the experimental value of equation (19)
see that this theoretical value is three orders of magnitude
o small to account for our observations.

rturbation theory

Now we calculate the cross section for multiphoton absorption
ing higher order perturbation theory. Following Gold and
bb[14] using a semiclassical formulation for the interaction
tween an atom and a radiation field of frequency ω and retain-
g only the lowest order nonvanishing $\vec{p} \cdot \vec{A}$ term, the transition

mplitude $a_f^{(N)}$ to a final state f from initial state g is given
n the Nth - order perturbation theory by

$$a_f^{(N)} = \hbar^{-N} \frac{\exp[i(\omega_{fg} - N\omega)t] - 1}{\omega_{fg} - N\omega} \sum_{m_{N-1}} \sum_{m_{N-2}} \cdots \sum_{m_1} \langle f | H_I | m_{N-1} \rangle$$

$$\frac{\langle m_{N-1} | H_I | m_{N-2} \rangle}{[\omega_{m_{N-1}g} - (N-1)\omega]} \times \cdots \times \frac{\langle m_2 | H_I | m_1 \rangle \langle m_1 | H_I | g \rangle}{[\omega_{m_2 g} - 2\omega][\omega_{m_1 g} - \omega]} .$$

ere the various m_i run over all the possible intermediate states
the atom whose energies with respect to the ground state are
$\omega_{m_i g}$. H_I is given by

$$H_I = \frac{-e}{mc} A_0 e^{i\vec{\eta}\cdot\vec{r}} \vec{\epsilon}\cdot\vec{p}$$

here $\vec{\eta}$ is the wave vector of the radiation, $\vec{\epsilon}$ the unit polariza-
ion vector and $\vec{p}$ the electronic momentum operator. Since the
pectral structure of bridging and nonbridging oxygens is not
nown, we do not assume the presence of any near resonances;
ather we assume that the intermediate state energies $\hbar\omega_{m_i g}$
ay be replaced by some appropriate average $\hbar\Omega$ independent
the state. With this approximation all the lower sums can be
illed out of the summation sign and the N summations can be
ollapsed down to one by using the closure properties of the
ntermediate states. The final state is approximated by a
lane wave of wave fector $\vec{k}$. Following Gold and Bebb,[14] the
otal cross section for the Nth order ionization becomes

$$\sigma_N = \frac{\left(\frac{2m}{\hbar}\right)^{3/2}(4\pi r_0 c)^N (N - \frac{\omega_0}{\omega})^{N+\frac{1}{2}} |M(f,g)|^2 S^{N-1}}{2\pi (2N+1)\omega^{-\frac{1}{2}} |\prod_{\lambda=1}^{N-1}(\Omega - \lambda\omega)|^2}$$

ere r_0 is the classical electron radius, $\hbar\omega_0$ the ionization otential and S the photon flux in photons cm^{-2} sec^{-1}. The atrix element $|M|^2$ between the ground state and the final lane wave state is approximated by $64\pi a^3$ where a is the atomic adius[14]; Ω has everywhere been set equal to ω_0 for the atom ecause the exact excited states of the nonbridging oxygens are ot known and the approximation made will appear reasonable for n order of magnitude estimate. Using this formula, the eoretical value for the cross section is

$$\sigma = 2.5 \times 10^{-30} \text{ cm}^2$$

n view of the approximations made, the agreement between xperiment and theory appears to be as good as could reasonably e expected, and we conclude that the photoconductivity we bserved is in fact due to multiphotonabsorption process ather than a high-field tunnelling mechanism.

It is important to note here that the photoconductivity bserved is a bulk phenomenon and does not arise from a few urface layers only. If the latter were the case, all of the lectron generation would have to take place with in about 0Å of the surface. Even with this generous assumption that ne surface effects dominate over such a large thickness, it ill require a multiphoton ionization cross section which is 10^6 times larger than predicted by the theory, and can not be ccounted for by any presently imaginable process.

CHAPTER VI

PLASMA FORMATION AND ENERGY ABSORPTION

All materials conduct electricity to a greater or lesser extent and all suffer some form of breakdown in sufficiently strong electric fields. The types of breakdown which solid dielectrics undergo can loosely be classified as intrinsic, thermal or avalanche breakdown.

The intrinsic breakdown occurs at low temperatures. The magnitude of the breakdown field strength is constant over a wide range of experimental circumstances such as the size and shape of the sample, or the material and configuration of the electrodes. This type of breakdown is called intrinsic, since it is regarded as being characteristic of the dielectric only at some given temperature. Since the breakdown field strength is not a function of the voltage waveform from d.c. to single impulses with microsecond rise times, it is inferred that the breakdown occurs in a time of the order of a microsecond or less. Intrinsic breakdown is observed in many dielectrics e.g. alkali halides, glass, mica and most polymers.

The experimental concept of thermal breakdown depends on the period of application of the applied voltage and there are two extreme cases: The first case is that in which the applied field is increased very slowly. Its chief characteristics are:

It occurs at high temperatures. The breakdown field strength depends on the size and shape of the sample, the geometry and thermal properties of the electrodes and the ambient medium.

The time required for breakdown is at least a millisecond and in most cases very much longer.

The other limiting case of thermal breakdown occurs when the field is applied rapidly. It is usually termed Impulse thermal breakdown and its distinguishing features are:

It occurs at high temperatures. Breakdown field strength does not depend greatly on the size and shape of the sample, but varies with the time of application of the field, being larger for an applied voltage pulse of short duration.

There is another approach to the problem of breakdown in which it is treated in the same manner as an electrical discharge in a gas. In its simplest form the theory of avalanche breakdown considers the conditions in which a single electron, or a few electrons, can cause an avalanche of electrons of sufficient size to destroy the insulating properties of the dielectric. If, at a given applied field, a single electron can succeed in producing another conduction electron by collisional ionization and these two produce two more etc., an avalanche of 2^i electrons will be produced in i generations. If the critical size for such an avalanche can be estimated, then a knowledge of the mean free path for collisional ionization would give the interelectrode distance required in order that such an avalanche may build up. This electronic instability must have thermal consequences, so neither intrinsic nor impulse thermal theory alone can completely explain the breakdown whose first step is the development of an electronic instability.

In the case of dielectric breakdown under high intensity laser radiation, where the high frequency voltage pulse is applied for a short interval of time (10^{-8} sec.), the complete process cannot be explained by the avalanche theory alone. The breakdown can be explained if the electronic instability is fully developed (i.e. there should be at least 10% of the atoms ionized) in a time much less than the pulse duration, the free electrons absorb sufficient energy from the remainder of the pulse and transfer it to the lattice to cause thermal breakdown.

At low intensities of the laser radiation it is shown in Chapter V that the free electrons may be produced by multiphoton ionization of the bridging as well as nonbridging oxygens in soda glass, fused quartz and quartz crystal. The number of free electrons liberated by the multiphoton ionization at the breakdown intensities (5×10^{9} W/cm^2) will be 2×10^{17} electrons/cm^3, or during the first quarter of the pulse duration there will be $\sim 5 \times 10^{16}$ electrons/cm^3 present in the focal volume. Thus at breakdown intensities there must be some multiplication of these electrons leading to a fully developed electronic instability (10^{19} - 10^{21} electrons/cm^3) in less than 10^{-8} sec.

Multiplication is also observed in the case of D. C. breakdown. Haworth and Bozorth[38] studied the D.C. prebreakdown phenomena in glass and observed a noisy prebreakdown current which grew so rapidly in magnitude that as the field was increased the breakdown current usually appeared as a discontinuity on this rising prebreakdown current.

This theory requires:

(1) Fields must be high enough that a single electron can pick up sufficient energy to cause collisional ionization.

(2) At breakdown fields of such short duration (2×10^{-8} sec), the electron density must reach a critical value to give rise to an effective absorption coefficient of at least 50 cm^{-1}.

In the next section we discuss the mechanisms by which the free electrons can absorb energy from the high frequency laser radiation.

CLASSICAL MICROWAVE THEORY OF BREAKDOWN

Minck and Rado[39] applied the classical microwave approach to the breakdown in gases under high intensity laser radiation. At laser intensities for which the photon density per mode is large, it is valid[40] to use the concept of an electric field. The energy transferred from the field to the electron can be derived by considering the motion of an electron accelerated by a harmonic field $E_o \cos \omega t$ and elastically scattered at frequency ν_c. The time average energy transfer per electron per second is

$$\frac{dW}{dt} = \frac{e^2 E_o^2 \nu_c}{2m(\omega^2 + \nu_c^2)} \qquad (1)$$

where e is the electronic charge, m the mass of the electron ω the laser angular frequency and ν_c the collisional frequency.

Relating E_o^2 to the intensity of the radiation field I by

$$I_0 = \frac{E_o^2 c}{8\pi} \tag{2}$$

we get

$$\frac{dW}{dt} = \frac{8\pi e^2 I \nu_c}{2mc(\omega^2+\nu_c^2)} \tag{3}$$

As well as gaining energy from the electric field, the electron communicates a fraction $\frac{2m}{M}$ of its energy to an atom of mass M at each collision. The the rate at which the electron gains energy is given by

$$\frac{dW}{dt} = \nu_c \left(\frac{4\pi e^2 I}{mc(\omega^2+\nu_c^2)} - \frac{2m}{M} W \right) \tag{4}$$

One usually assumes that ν_c is the frequency of elastic collisions, but strictly speaking the collision is not elastic since there is an exchange of energy with the radiation field. We will use an effective value of $\bar{\nu}_c$, which can be calculated from a consideration of the d.c. breakdown phenomenon in glasses as follows:

We calculate the value of $\bar{\nu}_c$, most appropriate to our problem from the experimental data on dielectric breakdown in glasses under voltage pulses of microsecond duration in which all the features can be explained by an avalanche theory of breakdown. In the single electron avalanche theory an electron

must pick up sufficient energy during a time $\tau(\equiv \frac{1}{\bar{\nu}_c})$ from the applied electric field to cause an ionizing collision at the end of the mean free life time τ. The rate at which the electron picks up energy from the applied electric field is given by

$$\frac{dW}{dt} = \frac{e^2 \tau E^2}{m} \qquad (5)$$

where E is the applied electric field. At the breakdown values of the applied field E_H, the increase in the electron energy ΔW during a time τ should be somewhat higher than the ionization energy to cause a collisional ionization of the oxygens in glass:

$$\Delta W (= W_o) = \frac{e^2}{2m} \tau^2 E_H^2 \qquad (6)$$

The breakdown will occur when the average electron is able to pick up energies of the order of W_o from the electric field in the time between two collisions. Seitz[41] pointed out that the experimentally observed value of the breakdown field E_B is determined not by the average behaviour of the electrons but by the fluctuations from this average. He calculated the effect of fluctuations, in which those electrons making no, or at the most a very small number of collisions form the important fraction which determines the breakdown. In these conditions the breakdown field E_B will at least be lowered to a value 0.2 E_H, where E_H is determined by assuming that the average behaviour of electrons is important. Even further lowering of the break-

down field will occur if the intermediate cases are involved. Thus the value $E_B = 0.2\ E_H$ may be viewed as giving a lower limit to the importance of fluctuations. Typical values of the breakdown field E_B for soda glass under pulses of micro-second duration are 11.5 MV/cm[42]. Rudenko and Tsvetkov[43] investigated the strength of dielectrics subject to nanosecond voltage pulses. The value of the breakdown field was found to vary slowly as the pulse duration was increased from 10 ns to 1 μ sec. For pulses shorter than 10 ns, the value of the break-down field increases sharply with the decreasing pulse duration. In view of these findings we take a value of E_B equal to twice the value obtained by Vermeer for a pulse duration of 10 n sec. Thus using E_B = 23 MV/cm, and E_H = 115 MV/cm and taking W_o = 7ev we get from equation (6) the value $\tau = 7.75 \times 10^{-16}$ sec. In appendix III we calculate the value of τ for different models of non-polar and polar dielectrics by considering the scattering of electrons by lattice vibrations. All those models are for idealized situations. In the case of glass where the scattering is enhanced on account of the impurities we should expect a much smaller value of τ. The above calculated value of $\tau (= 7.75 \times 10^{-16}$ sec) thus seems reasonable.

Using this value of τ, the electrons will pick up only 1.6×10^{11} ev/sec. even at the breakdown laser intensity of 5×10^9 watts/cm^2. As a result of collisions with the atoms it will also lose energy at the rate $\sim 10^{11}$ ev/sec. when its energy is near the ionization energy. Thus we see that the

electrons will lose energy at a significant rate and the avalanche will not be able to build up rapidly and this mechanism has to be ruled out.

ABSORPTION BY INVERSE BREMSTRAHLUNG

In the classical approach we calculated that an electron energy would change by the order of 10^{-4} ev during each cycle, whereas the energy of a ruby laser photon is 1.78 ev. While at microwave frequencies, using this approach, the electron energy change during each cycle of the applied field is of the order of the microwave photon energy. Hence any theory of breakdown at optical frequencies must be based on quantum mechanics as the classical theory is not applicable when the energy of each quantum is greater than the classical energy change. Here we consider a small number of electrons in the focal region of the laser beam produced by the multiphoton ionization. Each of these electrons gains energy from the radiation field by the inverse process of bremstrahlung, in which an electron can acquire the energy of a photon provided it is in the field of an atom or an ion, so that momentum may be conserved. This process is responsible for the absorption of photons by free electrons in the presence of atomic hydrogen in the photosphere of the sun[44]. In this way the electron energy builds up in a series of discrete steps. After accumulating an energy sufficient for ionization the electron ionizes the atom producing another free electron which begins the same process.

Cascade ionization of a gas at the focus of a laser beam is the subject of theoretical papers by Ya. B. Zeldovich and Raizer[45]; Wright[17], Ryutov[46], Askarayan and Rubinovich[47], Phelps[48], Browne[49] and Young and Hercher[50]. According to the general notions developed there the process proceeds as follows:

In the regions with large local fields, multiphoton ionization causes the first priming electrons to appear at the beginning of the laser pulse. These free electrons absorb light quanta by inverse bremstrahlung with the atoms or ions and ionize further collisonally. The energy of the electron in the random acts of interactions, changes alternately in one direction than in another so that the energy variation has in the main the character of a one dimensional diffusion along energy axis. The larger the quantum flux the faster this process. After accumulating an energy somewhat higher than the ionization potential the electron ionizes the atom with a high probability. As a result of this process one electron gives rise to two electrons with lower energy which begin the entire cycle anew. Quantum mechanical calculations of inverse bremstrahlung absorption rates as free-free transitions in hydrogen and noble gases are surveyed by Johnston[15]. A satisfactory treatment of free-free absorption in the field of ions other than hydrogen would require extensive numerical treatments using for example Hartree-Fock ionic states perturbed by the continuum of electronic states. As yet no such detailed treatments even for ions in gases (N_2, O_2 etc) are

available. In view of the lack of understanding about the status and the nature of electronic states and of ions in glasses we use the phenomenological approach of Wright[17] to obtain the free-free absorption rates in terms of the electron-atom collision cross section.

If there are N atoms/cm^3, S photons/cm^2 sec each of energy $\hbar\omega$ and n electrons/cm^3 at time τ, then the time for an electron travelling at a speed v cm/sec between successive scattering events by an atom is of order $\frac{\sqrt{\sigma}}{v}$, where σ(cm^2) is the electron atom collision crossection. The probability of a photon crossing the area σ during this time is,

$$S\ \sigma\frac{\sqrt{\sigma}}{v} \tag{7}$$

Since each electron is scattered $N\sigma v$ times per second, the rate of absorption of energy by each electron is

$$\begin{aligned}\frac{dW}{dt} &= NS\sigma^{5/2}\hbar\omega \\ &= NS\hbar\omega\phi_a\end{aligned} \tag{8}$$

where $\phi_a(\equiv \sigma^{5/2})$ is the free-free absorption cross section per atom. Here we are only considering the absorption of photons when electrons are scattered in the field of the atoms.

There is another important mechanism for the acceleration of electrons, namely that of inverse bremstrahlung absorption in the field of the ions. A convenient though rough measure of the relative importance of ions in the free-free transitions

is provided by the work of Firsov and Chibisov[16]. The ratio of the two cross sections is given by

$$\frac{\phi_i}{\phi_a} = \frac{2.2 \times 10^3}{\theta^2 \sigma \left[4 + 3\frac{h\nu}{\theta}\right]} \tag{9}$$

where ϕ_i is the free-free absorption cross section per electron per ion, σ is the elastic scattering cross section in units of 10^{-16} cm^2, θ is the electron temperature in ev and $h\nu$ is the photon energy. Using a value of θ equal to the average electron energy i.e. $\theta = 3$ ev., we get from (9)

$$\frac{\phi_i}{\phi_a} = 10 \tag{10}$$

The rate of absorption of energy by each electron in the field of ions will be

$$\frac{dW}{dt} = N_i S \hbar\omega \phi_i = N_i S \hbar\omega \times 10 \sigma^{-5/2} \tag{11}$$

where N_i is the density of ions. Because of the low density of ions, this process will not be important in the initial stages of the development of breakdown.

While electrons are gaining energy by the inverse bremstrahlung mechanism, they are also losing energy by elastic collisions with the lattice. The average rate of loss of energy to the lattice from each electron is given by

$$\frac{dW}{dt} = -N v \sigma \frac{2m}{M} \overline{W} \tag{12}$$

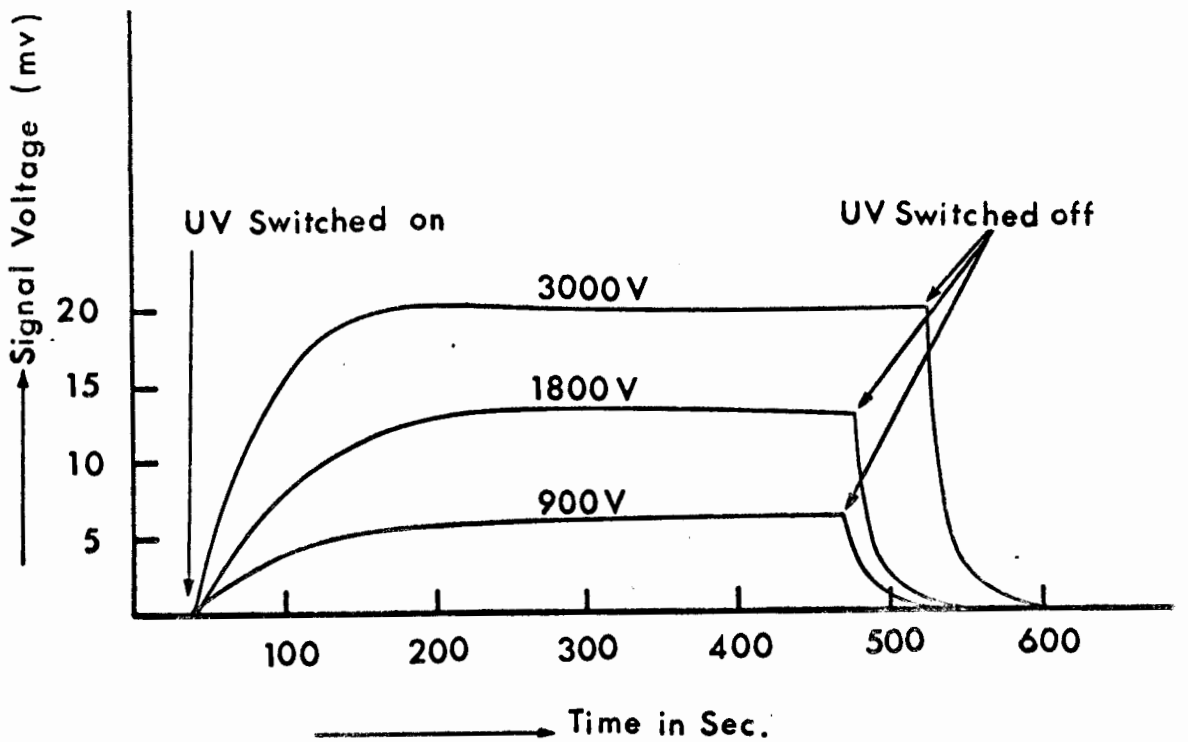
Signal Voltage (mv)
20
15
10
5
UV Switched on
UV Switched off
3000 V
1800 V
900 V
100
200
300
400
500
600
Time in Sec.

Fig. 6.1

where $\overline{W}$ is the average electron energy which is equal to half of the ionization energy. From (8) and (12) we can calculate the value of the photon flux at which the average rate of gain of energy is balanced by the average rate of loss. Equating (8) and (12) we get

$$S = \nu \frac{2\overline{W}}{\hbar\omega} \cdot \frac{m}{M} (\sigma)^{-3/2}$$
$$= 1.24 \times 10^{27} \text{ photons/cm}^2 \text{ sec.} \qquad (13)$$

Thus we see that for a photon flux of 1.24×10^{27} photons per sec cm^2 (or 4×10^8 W/cm^2) the average electron will not gain enough energy from the radiation field to cause collisional ionization and thus the threshold intensity for the dielectric breakdown will have to be higher than this value.

THE EFFECT OF INITIATING ELECTRONS AND ELECTRON MULTIPLICATION

To study the effect of primary electrons on the breakdown threshold and to investigate the threshold for electron multiplication we performed the following experiments.

Photoconductivity in soda glass was observed by Rohatgi[13] under irradiation by light of wavelength 2537Å. We used a high pressure mercury arc lamp to produce the initiating free electrons. Photoconductivity response in our examples at different collecting voltages is shown in figure 6.1. From the steady state value of the photocurrent and using the value of electron mobility obtained by Rohatgi, we estimated that 2×10^{12} free electrons/cm^3

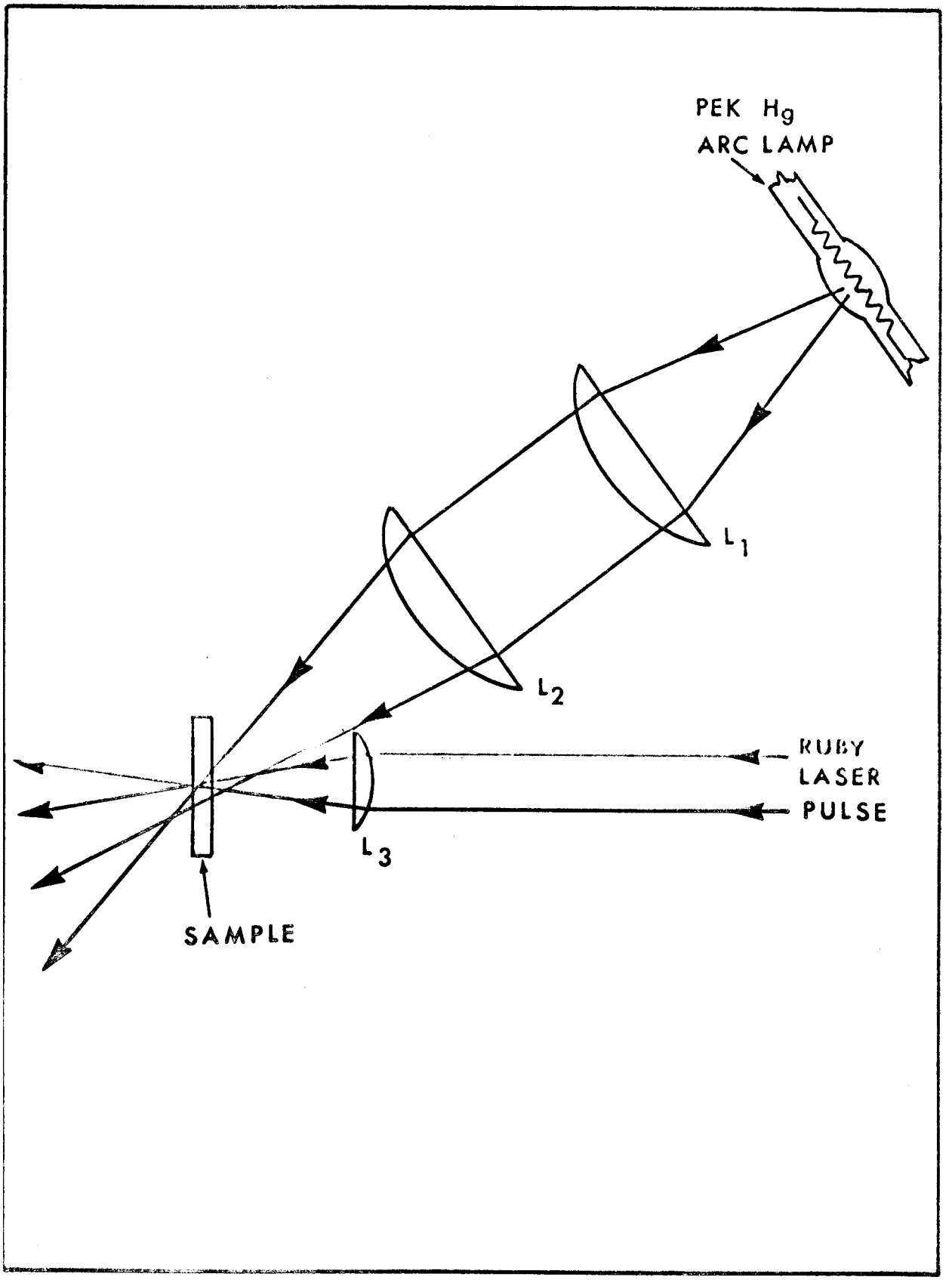

Fig. 6.2 L_1 - Quartz Lens f = 75 mm.
L_2 - Quartz Lens f = 100 mm.
L_3 - Glass Lens f = 100 mm.

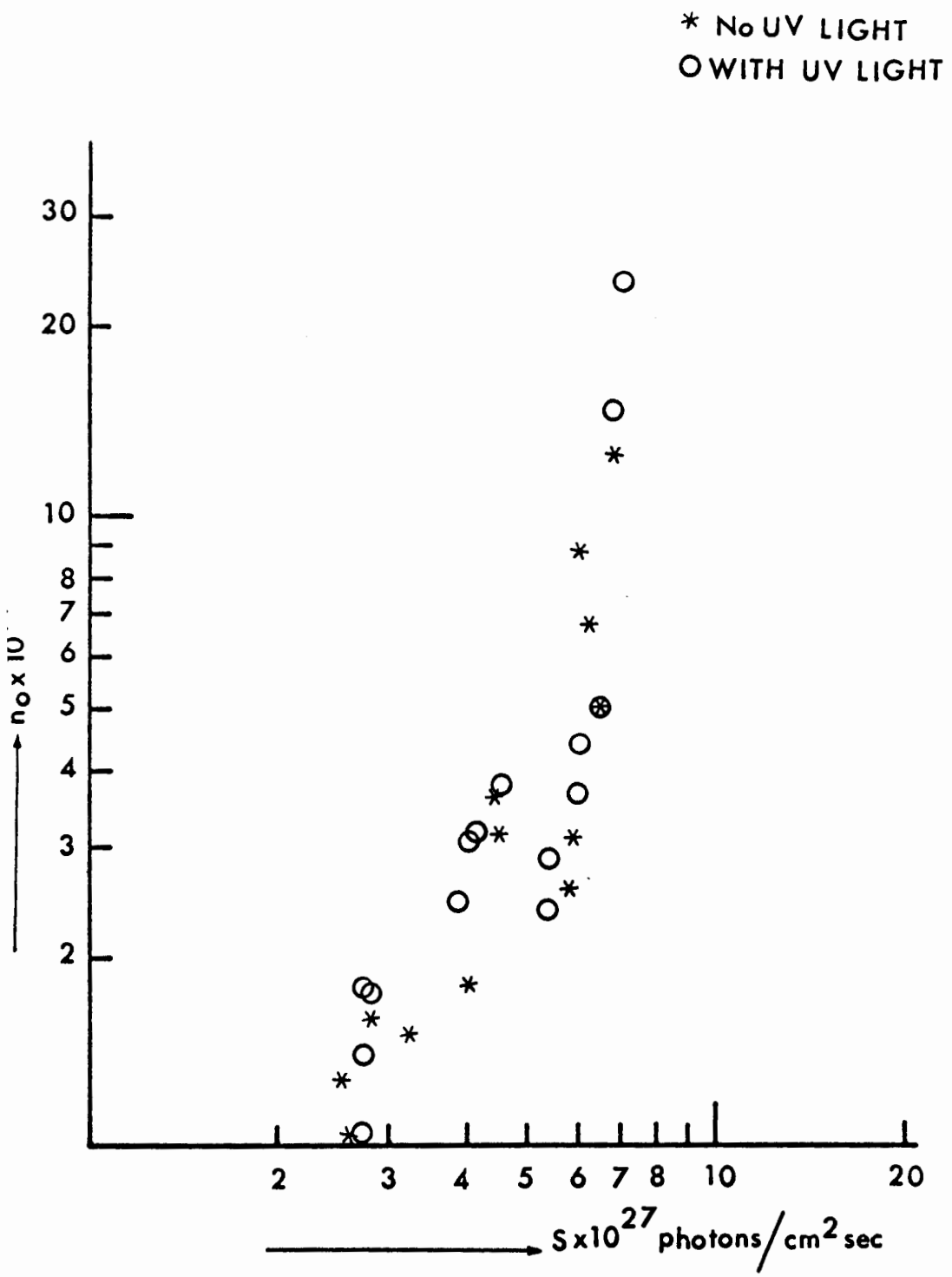
* No UV LIGHT
O WITH UV LIGHT
30
20
10
8
7
6
5
4
3
2
$n_o \times 10$
2
3
4
5
6
7
8
10
20
$S \times 10^{27}$ photons/cm^2 sec

Fig. 6.3

are produced at this excitation intensity used. If there is some multiplication of electrons due to the free-free absorption in the field of the atoms, than at low intensities, where the ion density is low, these primary electrons produced by the ultraviolet light should absorb energy and give rise to a multiplicative process. To check this we monitored the photo-conductivity signal with the ultraviolet light on and also with the ultraviolet light off. The experimental arrangement is shown in figure 6.2. Ultraviolet light from a 200 W mercury lamp is focused on the front face of the sample using quartz optics. The size of the uv focal spot was 300 times the size of the laser focal spot. The number of electrons generated by the laser pulse is estimated in the same fashion as discussed in chapter 5. The photoconductivity pulse shape was the same in both cases. The number of electrons generated in the soda glass as a function of the incident laser intensity is shown in figure 6.3, for the cases when the uv light is on and when it is off. From the graph we note that up to the incident flux densities of $5 \times 10^{27} \frac{\text{photons}}{\text{cm}^2 \text{sec.}}$ there is no multiplication occuring. Between 5 to 6 $\times 10^{27}$ photons/cm^2 sec. we notice a sharp increase in the photoconductivity signal. It is of interest to note that no visible damage to the glass sample was observed at these intensities. While at intensities higher than this the photoconductivity signal is many orders of magnitude larger and mechanical damage is also observed.

The overlap between the points obtained when the ultraviolet

light is on and when it is off should be noted. We did not observe any increased electron generation by the laser pulse when 10^{12} electrons/cm^3 are present. At the intensities where some multiplication is observed, there will be about 10^{14} electrons/cm^3 produced by multiphoton ionization, so the role of 10^{12} electrons/cm^3 produced by the ultraviolet light is masked. To verify that this is in fact the case we checked the effect of uv light on the threshold intensity for breakdown in soda glass. The threshold intensity with the uv light on was found to be (2-5) x 10^9 watts/cm^2 and with no uv light it was (3-5.5) x 10^9 watts/cm^2. The large scatter in this data is attributed to thermal and elastic inhomogeneities in the material. For laser induced breakdown in gases Young and Hercher[50] did not see any difference in the breakdown threshold in helium or argon with an external source of ionization.

ABSORPTION OF RADIATION IN THE FOCAL VOLUME

We have seen that the net rate of gain of energy by an electron by free-free absorption in the field of an atom is

$$\frac{dW}{dt} = N S \sigma^{5/2} \hbar\omega \left(1 - \frac{2\nu W m}{S \sigma^{3/2} \hbar\omega M}\right) \qquad (14)$$

Since σ is a function of energy it is not possible to integrate this equation analytically. At the breakdown photon densities ($2\nu Wm/S\sigma^{3/2}\hbar\omega M$) is appreciably less than unity and we replace this quantity by the appropriate mean value. Integrating (14)

one finds the time t_d to attain the excitation potential energy W_o from some low value of energy is

$$t_d = \frac{W_o}{NS\bar{\sigma}^{5/2}\hbar\omega\left(1 - \frac{vW_o m}{S\bar{\sigma}^{3/2}\hbar\omega M}\right)} \quad . \tag{15}$$

where $\bar{\sigma} = 4.3 \times 10^{-16}$ cm^2 and $\frac{W_o}{\hbar\omega} = 4$. At incident photon flux densities of 1.24×10^{28} photons/cm^{2}sec., t_d will be equal to 3×10^{-12} sec. and in a time less than a nanosecond the focal region will be completely ionized. Now if ϕ_a is the absorption cross section for free-free absorption in the system (electron + atom) and ϕ_i is that for the system (electron + positive ion), then the linear absorption coefficient for the glass in the focal volume is

$$\xi = N_e(N\phi_a + N_i\phi_i) \quad . \tag{16}$$

where N, N_i and N_e are the density of atoms, ions and electrons respectively. It was shown earlier $\phi_i \simeq 10\,\phi_a$ and since in less than a nanosecond most of the atoms are ionized, the effective absorption coefficient becomes

$$\xi = N_e N_i \phi_i \quad . \tag{17}$$

Substituting the values of $N_e = N_i = 10^{22}$, and $\phi_i = 10\bar{\sigma}^{5/2}$ we get

$$\xi = 10^6 \text{ cm}^{-1}.$$

So we see that at flux densities above the threshold for breakdown there will be very strong absorption. This strong absorption has been noticed by many workers in this field[7,19] and shows itself as a complete absorption of the laser pulse. A trace of the incident and transmitted pulse shape is shown in figure 2.1. This attenuation of the incident pulse is partly due to the strong scattering by the free electrons. Dupont, et al.[19] observed that about 3% of the incident radiation was scattered in the forward direction in the case of laser induced internal damage in borosilicate glass. Young, et al.[61] found similar results in the case of laser induced breakdown in air. No such attenuation or scattering of the pulse is observed at intensities below the threshold for breakdown.

The phenomenon under consideration is unique in that the rate of heating is so rapid that diffusion or recombinations do not have time to occur. The electron loss due to diffusion drift from the beam focussing volume will decrease the electron density at a rate $\frac{N_e}{\tau_D}$, where τ_D is the average time an electron stays in a volume of radius r. This time is approximately equal to $\tau_D = r^2/(\frac{v^2\tau}{3})$ where τ is the electron scattering time. For the electrons of interest $v \simeq 10^8$ cm/sec. $\tau = 7.75 \times 10^{-16}$ sec. and $r = 10^{-3}$ cm one obtains $\tau_D = 4 \times 10^{-6}$ sec. Thus even during the full duration of the laser pulse (10^{-8} sec.) most of the electrons will stay in the focal region. The mean free life time of these electrons is 10^{-5} sec., thus recombination will not affect the electron density either.

Thus it is shown that for photon densities less than 2×10^{27} photons/cm^2 sec., ($\simeq 6 \times 10^8$ W/cm^2) there will not be any multiplication or strong absorption of the laser radiation in the focal volume. While for photon densities of the order of 1.2×10^{28} photons/cm^2sec, (5×10^9 W/cm^2) the electronic instability will be fully developed within the first few nanoseconds and strong absorption will occur. The experimentally observed value of the breakdown threshold is $(3\text{-}5) \times 10^9$ W/cm^2. It should be noted that a breakdown threshold of less than 6×10^8 W/cm^2 has never been reported in the literature. In the case of fused quartz and quartz crystal, the breakdown threshold is found to be higher than glass. This increase in the breakdown threshold can be explained by considering the effect of the electron scattering cross-section on the threshold intensities. It was established in Chapter V that electrons are liberated in glass, fused quartz and quartz crystal by the four photon ionization. These primary electrons are then accelerated by the inverse bremstrahlung absorption mechanism and breakdown threshold is determined by the average rate of loss of energy. From equation (13) we see that the breakdown threshold is proportional to $\sigma^{-3/2}$. The value of σ most appropriate to our problem was obtained from the considerations of the D.C. breakdown experiments. Using equation (6) in (13) we get

$$P_{damage} \propto E_B^{-3/2} \qquad (18)$$

where P_{damage} is the threshold power density for damage and E_B is the experimentally observed value of the d.c. breakdown

field. Values of the intrinsic breakdown field in glass, fused quartz and quartz crystal at room temperature are 9.2 MV, 7MV and 5MV per cm. respectively. Thus from this data we would expect the damage threshold in fused quartz and quartz crystal to be higher by factors of 1.5 and 2.5 respectively which is in fair agreement with the experimentally observed values of Ritus and Manenkov[26].

Thus we see that multiphoton ionization is capable of providing initiating electrons. These primary electrons pick up energy from the radiation field of the laser pulse by the inverse bremstrahlung process and multiply. The breakdown threshold is determined by the rate of absorption of energy by the above mentioned mechanism and the rate of loss of energy due to elastic collisions with lattice. At intensities above the threshold the rate of gain of energy will exceed the rate of loss of energy by at least a factor of ten and electrons will rapidly gain energies higher than the ionization potential, leading to fully developed instability in few nanosecond.

At these electron densities the laser beam is strongly absorbed in the focal volume. The diffusion and recombinations are found to be very slow and do not affect the electron multiplication process. Due to the multiphoton ionization, the effect of an external source of ionization is masked.

CHAPTER VII

FURTHER WORK, DISCUSSION AND CONCLUSIONS

During this investigation of the damage mechanism in silicate glasses many interesting observations were made. Some of these lead to a whole complex of new questions as to the details of the electron recombinations, the effect of the primary electrons on the optical properties of glass and on the cascade development, etc. Thus a few suggestions for further work may be appropriate here.

(i) Enhancement of Photoconductivity

Earlier in Chapter V it was described how photoconductivity can be induced in silicate glasses by high intensity radiation from a ruby laser. The photoconductivity signal was found to vary roughly as the fourth power of the laser intensity. At intensities below the threshold for breakdown, there were no physical or structural changes caused as was evidenced by the reproducibility of the photoconductivity signals taken at intervals of 3 to 5 minutes and in room light. When the ruby laser operated with a passive chemical Q-switch was pumped sufficiently high above the threshold, a double laser pulse was obtained with a time separation of $1.5\text{-}3 \times 10^{-4}$ seconds. The second pulse was usually of higher intensity than the first. Using the experimental arrangement shown in Figure 5.1, the photoconductivity induced by such double pulses was studied. On account of the intensity dependence of the photoconductivity signal, the second pulse always

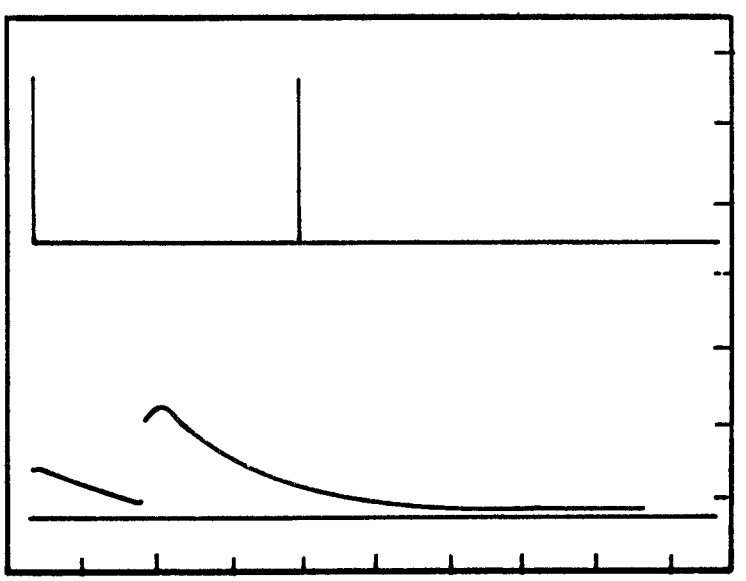

Fig. 7.1

Upper trace laser pulses 50μ sec/div., .005V/div.
Lower trace .05V/div., 0.1 m sec/div.

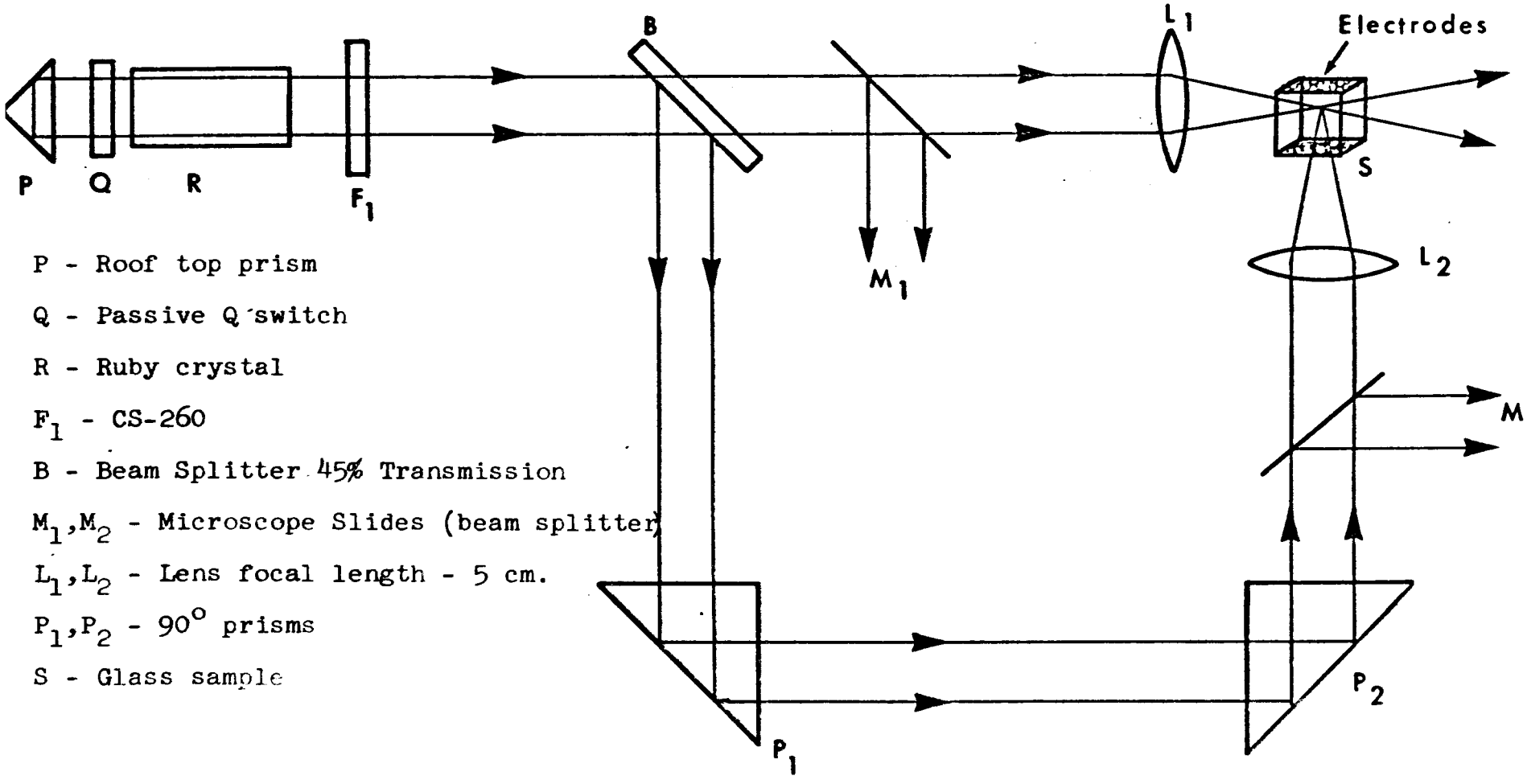

P - Roof top prism

Q - Passive Q switch

R - Ruby crystal

F_1 - CS-260

B - Beam Splitter 45% Transmission

M_1,M_2 - Microscope Slides (beam splitter)

L_1,L_2 - Lens focal length - 5 cm.

P_1,P_2 - 90° prisms

S - Glass sample

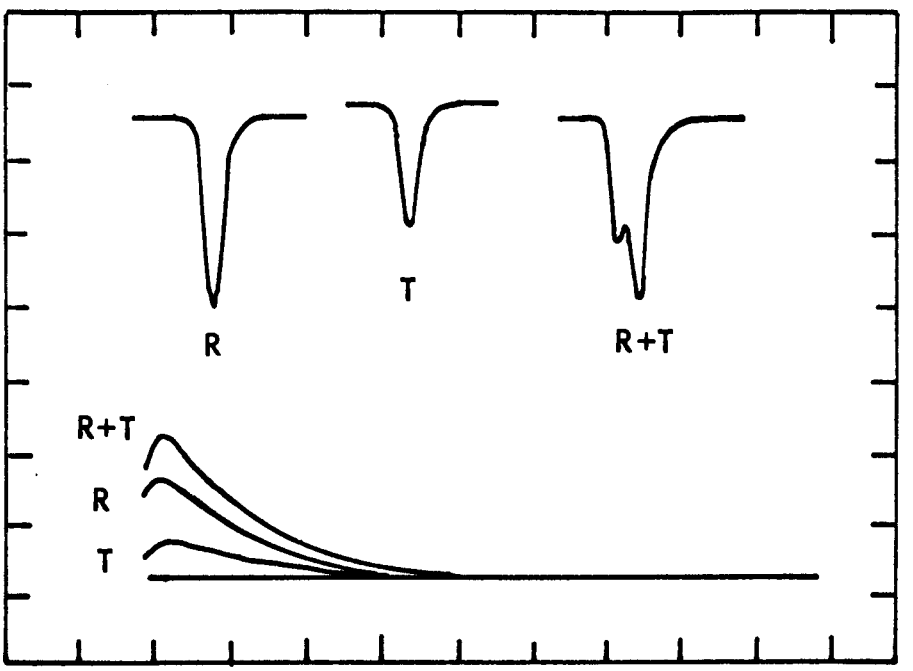

Fig. 7.3 Upper trace 100 ns/div., 5 mV/div.
Lower trace 0.1 m sec/div., .05 V/div., amplification 20.
Delay between pulse $\approx$ 25 ns
R - Reflected pulse, T - Transmitted pulse
(T+R) Reflected and Transmitted.

yielded a higher signal than the first. The excess number of electrons generated by the second pulse could not be accounted for wholly on the basis of this intensity dependence. Figure 7.1 shows the effect of a double pulse on the photoconductivity signal. The upper trace is the laser output. The laser was pumped above the threshold to give two pulses 3×10^{-4} sec. apart. Each pulse has a peak power of 2.7 MW and a duration of 40 n sec. The lower trace is the photoconductivity signal, the first sharp rise was the result of the first laser pulse and the second sharp rise resulted from the laser pulse arriving 3×10^{-4} sec. later. The shape of the photoconductivity signal is the same in both cases. Even though the peak power in both pulses is equal, the second laser pulse produced almost twice as many electrons as the first one. There was no dependence of the excess number of electrons generated on the time delay between the pulses in the range from 5×10^{-5} to 5×10^{-4} sec. However, when a single pulse was split into two parts by a beam splitter and brought to the sample after a delay of about 24 n sec. had been introduced between the parts by the arrangement shown in Figure 7.2, no enhancement of photoconductivity was observed. Figure 7.3 shows three photoconductivity signals obtained by a reflected laser pulse, a transmitted laser pulse and the third one by combining the two. It was also noticed that in the presence of light from a mercury arc lamp the enhancement otherwise observed in a second pulse will disappear.

These results can be understood qualitatively by considering the recombination mechanism of the electrons. Free electrons created in glass by ultra-violet light or X-rays or by the multiphoton ionization are trapped by impurities and give rise to color bands. These color bands can be bleached by shining light in the visible region of the spectrum onto the glass. In the single pulse photoconductivity experiments, color bands were bleached by room light at room temperature in times of the order of 3 to 5 minutes. In the double pulse experiments where the second pulse comes within less than a milisecond of the first one, not only are electrons removed from the bridging and nonbridging oxygens but also from the color-centers (and with greater efficiency on account of the reduced energy requirement) thus liberating the additional number of electrons observed. If the second pulse arrives within a few nanoseconds of the first pulse, electron free life time being 10^{-5} sec. there will be as yet no significant number of electrons trapped by the impurities, and consequently there is no enhancement. The presence of light from a mercury arc lamp bleaches these color bands immediately thus eliminating the contribution from impurities under these circumstances at any time. It is important to note that with the laser intensities used in these observations no multiplication of electrons was observed.

A similar observation was made in fused quartz.

For the complete understanding of the recombination

mechanism of the electrons generated in glasses and the possibility of some short lived microstructural changes induced by the subthreshold laser pulses, more work should be done along the following lines:

(1) Enhancement of the photoconductivity signal should be studied at different temperatures and for the complete range of time delays from 10 ns to 10^{-4} sec.

(2) An electron microscope should be used to study the possibility of microstructural changes induced by the laser pulse below the threshold for macroscopic damage.

(ii) Induced Change in Refractive Index

To estimate the contribution of free electrons generated by the multiphoton ionization in a glass to its refractive index we tried the following experiment.

When a light beam strikes the boundary from the side of an optically dense medium, the transmitted light is a function of the angle of incidence. Near the critical angle of incidence the transmitted intensity is a strong function of the refractive index. This fact was exploited to measure the small induced change in the refractive index of glass at high intensities. Using a He-Ne gas laser as a source for the reference beam we observed a decrease in the transmitted intensity when a 3.6 MW, 40 n sec. ruby laser pulse was focused on the same spot where the reference beam emerged

from the glass sample filled with a liquid of matching index of refraction. This decrease in the reference beam intensity was not coincident with the laser pulse and after about 100 n sec. it returned back to normal level. No mechanical damage was observed at the surface. This decrease in the reference beam's transmitted intensity when translated into the corresponding change in the angle of refraction yielded a value for $\frac{\Delta n}{n_o} = 4 \times 10^{-4}$ where n_o is the ordinary refractive index. This is a rather large change in refractive index. At the intensity of the ruby laser pulse used, the contribution from electrostrictive effects will be $\sim 10^{-7}$ and from the free electrons generated by multiphoton ionization will be 10^{-8}. If the glass sample was heated up and the change was due to temperature rise, we will expect the transmitted signal to stay at the decreased level for a much longer time, because of the low thermal conductivity of glass. The large change in $\frac{\Delta n}{n_o}$ deduced above only on the basis of the effects in glass may however be due to the changes occuring in the liquid used inside the sample. This line of investigation was not pursued any further since the main interest in this work was the damage mechanism. However to study the change in refractive index with this method, we propose that solid prism should be used. Monitoring the change in refractive index by the above mentioned technique one can study the induced polarization at different wavelengths which is given by

$$P(w) = \chi^{NL} (E_{w_1})^2 E_w$$

where E_{w_1} is the incident laser electric field and χ^{NL} is the nonlinear susceptibility of the media and E_w is the electric field of reference light beam. The study of the induced polarization should help in determining the contribution from the free electrons generated by multiphoton ionization.

(iii) Estimation of Surface Energy of Glass

Surface energy of a solid or a liquid phase of a substance is defined as the amount of work done to increase its surface by one square centimeter. In principle, any experiment which changes the surface area of the material can be used to derive its surface energy if the amount of energy spent for this change in surface area can be measured. We estimated the surface energy of soda glass using a ruby laser pulse of intensity above the threshold for breakdown to create new surface in the bulk material. The amount of incident energy absorbed to cause fracture can be estimated from the known attenuation of the incident laser pulse. Since the thermal stresses set up within the material develop very fast we assume that the losses due to plastic flow are negligible. Comparison of the spectrum of the radiated energy with a black body leads to an estimate of the temperatures reached in the focal volume. Knowing this

temperature, the radiation and conduction losses can be estimated. Thus one can compare the energy absorbed with the energy used in creating new surfaces within the material

$$E_{absorbed} = E_{radiated} + E_{conducted} + \gamma A$$

where γ is the surface energy and A is the amount of surface area created. Using this approach we obtained a value of $\gamma = 10^5$ ergs/cm^2 for soda glass. This agrees well with the values obtained by crushing techniques.

(iv) Effect of Primary Electrons on the Breakdown Threshold

It was shown in Chapter VI that the diffusion and recombinations do not affect the development of the electron cascade, only the loss of energy by elastic collisions controls the electron doubling process and hence the threshold for breakdown. We suggest the use of certain crystals where the electron-atom collision cross section is relatively small but the ionization potential is low enough to generate sufficient number of electrons by multiphoton ionization to give rise to an effective absorption exceeding that required from thermoelastic considerations. Thus the breakdown threshold in such a case will not be determined by the electron doubling process but by the multiphoton ionization. Some of the semiconductor crystals may qualify for this such as CdS or ZnTe, maybe used.

(v) Conclusions

From the discussions of the preceding chapters one can arrive at the following summary of definite and tentative conclusions:

(1) Dielectric breakdown and mechanical damage is caused in transparent materials at laser intensities of $5 \times 10^{9} - 10^{11}$ watts/cm^{2} due to the failure of material to withstand the thermal stresses set up by the nonlinear absorption of the laser radiation. An effective absorption of 50 cm^{-1} must occur in the focal volume to generate thermal stresses of destructive magnitude. The residual linear absorption of the material, direct light pressure of radiation or electrostrictive pressure or the stimulated Brillouin scattering of the laser radiation cannot account for the effective absorption or the stresses required to cause mechanical damage and hence are ruled out as possible mechanisms.

(2) It is established that even at laser intensities below the threshold for damage photoconductivity is induced in silicate glasses. The number of free electrons generated are accounted for by the multiphoton ionization of bridging and nonbridging oxygens in the silicon oxygen network. The mean free life time of these electrons is 10^{-5} sec. At laser intensities above the threshold for breakdown, these electrons absorb energy by an inverse bremstrahlung process. The cross section for the inverse bremstrahlung absorption in the field of ions is ten times more than in the field of the atoms.

Since the density of ions is small in the initial stages of the build up, electrons are mainly accelerated by inverse bremstrahlung absorption in the field of the atoms only. The rate at which the electron density builds up is governed by the rate of loss of energy to the lattice via elastic collisions, recombination and diffusion being negligible. At the intensities where the rate of gain of energy exceeds the rate of loss of energy by an average electron, the multiplication of electrons takes place at a rapid rate, and within few nanoseconds, the focal volume is completely ionized. After this stage the free electrons absorb the incident radiation strongly and inverse bremstrahlung absorption in the field of ions leads to absorption coefficients of the order 10^{+6} cm^{-1}. The absorbed energy is used in heating up of the lattice, and this sudden heating gives rise to thermal stresses far exceeding the strength of the glass involved. The variation in the threshold intensity for breakdown in different glasses is due to the variation in electron-atom collision cross section.

(3) Free electrons produced in the glasses are trapped by the impurities and if a second laser pulse comes within 10^{-5} to 5×10^{-4} sec. of the first pulse, it ionizes not only the bridging and nonbridging oxygens but also impurity atoms thus leading to an enhancement of the photoconductivity signal.

(4) A direct method for the estimation of surface energy of glasses and other transparent materials is given and the surface energy of glass is found to be 10^{5} $ergs/cm^{2}$.

APPENDIX I

STRUCTURE OF GLASS

The glassy state is a particular case of the amorphous state of matter, attained under certain conditions in the transition from the liquid to the solid state. The number of glass forming systems and the variety of possible structures are tremendous, especially if we adopt the definition that any solid substance which has a structure without long range order is a glass. It is more usual to impose the additional restriction that the solid should be obtainable by quenching a certain amount of melt; if no crystallinity could be detected by optical inspection or by X-ray diffraction, the sample would by definition be a glass. We will restrict our considerations only to silicate glasses such as fused quartz and alkali silicate glasses.

Glass appears to have many of the features of a normal solid, such as strength, hardness, etc., but closer examination shows that contrary to crystalline solids it has an extended melting range and X-ray analysis indicates a molecular structure akin to that of a liquid at low temperature. Zachariasen[51] proposed that the atomic or molecular arrangement in the glass like state is an extended network which lacks symmetry and periodicity. He laid down a number of simple rules relating the way, the oxygen anions and cations must link together to form an oxide to exist in the glassy state. Briefly, the glass forming cations (e.g. B^{3+}, Si^{4+}, P^{5+}) are surrounded by polyhedra of oxygen ions in the form of triangles or tetrahedra. The oxygen ions

are of two kinds viz bridging oxygen ions (which link two polyhedra) and nonbridging oxygen ions, each of which belongs to only one polyhedron. Such a system will produce a polymer like structure with long chains crosslinked at intervals. In such a structure there are regions of unbalanced negative charge where the oxygen ions are nonbridging. Cations of low positive charge and large size (e.g. Na^+, K^+, Ca^{++}, Mg^{++}) may exist in holes between the oxygen where they compensate the excess negative charge of the nonbridging oxygen ions. Oxides forming the basis of a glass are known as network formers and those which are soluble in the network are termed as network modifiers. Some oxides cannot be easily classified in this way and are termed intermediates. Sun[52] advanced a theory that glasses are only formed from those oxides in which the bond strength between the oxygen and the cation reaches a certain minimum value. Oxides with lower bond strength may act as network modifiers or intermediates and not as network formers. The bond strength (M ⟷ O) of all glass formers is greater than 80 Kcal. per Avogadro bond, that of intermediates (60 - 80) Kcal and of modifiers less than 60 Kcal per Avogadro bond. This transition is continuous and the classification is somewhat arbitrary.

The glassy state is attained under certain conditions in the transition from the liquid to solid phase. Together with enforced undercooling of a substance in the liquid state below the melting point, glass formation is favored by high viscosity which according to Tammann[53] hinders the crystallization process

which necessitate the total regrouping of the particles. This high viscosity is physically determined by the long relaxation times of the atomic processes in the corresponding liquid systems. In the processes taking place in condensed systems it is necessary to take into account the force constants characterizing the rigidity of the bonds between atoms and ions. In substances of ionic structure, there is appreciable diffusion of ions in the crystal and the expansion coefficients are high. These processes require low activation energies. Activation energies are lowered owing to the overlapping of the long range electrostatic coulomb fields created by the combination of ions in a condensed system. It follows that in glasses reduced fluidity and relatively low expansion coefficients are attributable to the predominance of short range localized covalent bonds between the atoms. This prevents transitions of the structural elements in the melt into the state of complete readiness for crystallization thus favoring the formation of glass.

X-ray diffraction experiments also tell us about the nature of the chemical binding forces[54]. In the case of pure fused silica (SiO_2), it is incorrect to talk of Si^{4+} and O^{2-} ions since X-ray diffraction experiments show that the nuclei of oxygens are surrounded by a lower electron density than that would correspond to the quantum state O^{2-}. The electron density around the silicon is higher than that would correspond to si^{4+}. This deviation from the ideal ionic structure has been attributed to partial covalency meaning that the quantum state is somewhere

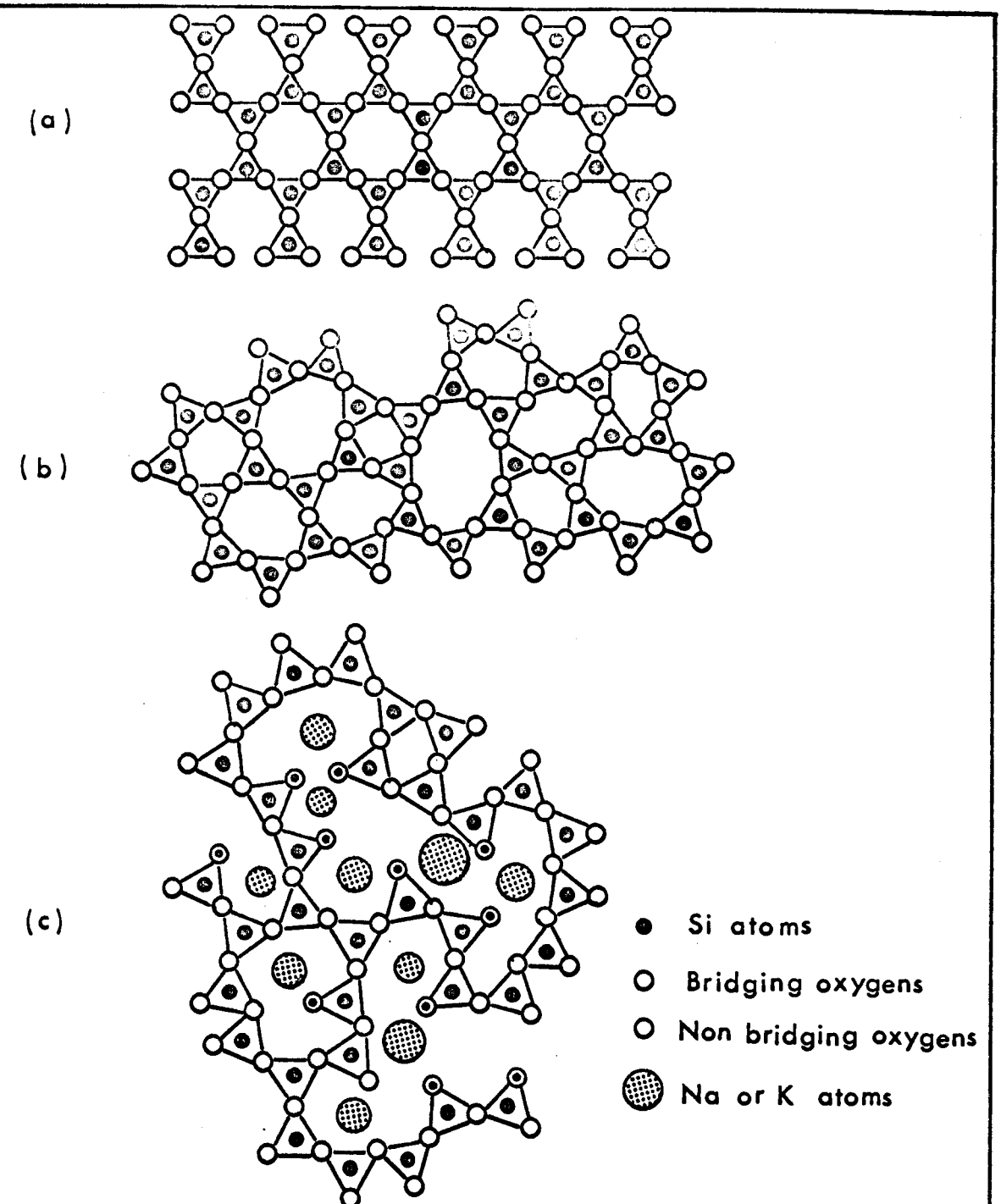

Fig. I.1 Schematic two-dimensional representation of
(a) Quartz crystal (b) Fused quartz
(c) Soda glass

between ions and neutral atoms. The anomalously small distance (1.60Å) between Si - O atoms is the result of the shortening of the ionic bond by partial covalency.

The structure of silicate glasses is determined by the presence of Si-o-Si bonds. Uni and bivalent cations form purely ionic bonds and tend to b e surrounded by coordination polyhedra of single bonded oxygen ions. Thus in the case of typical sodium silicate glass, the silicon atoms are surrounded by oxygen tetrahedra. Some of the oxygens are nonbridging. The sodium ions are held in the various holes in the Si-O network and are surrounded on the average by six oxygen atoms. A two dimensional structure of the soda glass and fused quartz is shown in figure I.1. Increasing the alkali metal component in glasses has a marked effect on the network stiffness and hence the mechanical properties. Because of their tendency to be surrounded by nonbridging oxygens, increase of alkali content will increase the number of nonbridging oxygens.

Electrical Properties:

Pure silica is one of the best electrical insulators with a volume electrical conductivity as low as 10^{-18} ohm^{-1} cm^{-1} and it is very likely that even this low conductance is not intrinsic but is a result of unavoidable contaminations. This high insulating power of pure silica is the result of two factors. All binding forces are strong and the glass contains no major concentration of singly charged ions. In complex glasses such

as sodium silicate glass the conductivity is primarily the result of Na^+ migration. Sodium ions are the most mobile components of glass where as O^{2-} ions with which they are associated in Si - O random network are not mobile at normal temperatures. Thus if electrical conduction by alkali ions occurs it will gradually cease as the alkali ions migrate in the glass and a negative space charge grows at the anode while a Na^+ space charge grows at the cathode. The electrical conductivity of glass increases as the temperature is raised because of the greater ease with which the ions can move when thermal agitation has weakened the forces binding them to the silica network.

Transparency of Glass:

The electrical nature of glass which lacks electronic conductivity on account of the tight binding of the electrons in the structure, is responsible for the lack of interaction with an electromagnetic wave in the visible region of the spectrum. Perfect crystals of an ionic (NaCl) or covalent nature with strongly bound electrons are transparent. On the other hand crystals which have metallic bonding are opaque due to the presence of free electrons. Elements such as copper, cobalt, chromium, iron, nickel, manganese, etc. produce deeply colored glasses. Such colored glasses also possess some transparency. The exact reason for the appearance of colors is connected with the valency and valence change, polarization effects and

chemical as well as electrical nature of these compounds. Thus the blue color of iron glasses containing both divalent and trivalent ions is the result of an electronic transition involving two ions of the same element but different valency.

APPENDIX II

NOTE ON THE STRENGTH OF GLASS

At ordinary temperatures glass can respond to mechanical forces in different ways described as its elasticity, delayed elasticity and fracture. Elasticity involves reversible changes of some interatomic distances: Particles return to their original positions as soon as the applied stress is released. At low temperatures (< 400° C) glasses obey Hooke's law.

Most glasses also show the phenomenon of internal friction or delayed elasticity: Response to the applied stresses is not instantaneous, time is required for some atoms to reach new equilibrium positions when stress is applied as well as when it is released. This phenomenon arises when the new equilibrium positions are separated from the original ones by energy barriers of the order of kT.

Fracture differs from elasticity inasmuch as it is an irreversible process. It is the most important property of glass from engineering as well as our point of view. In glasses the amount of permanent deformation preceding fracture is negligible and it is termed "brittle" fracture. Fracture is linked to a number of mechanical properties, such as elasticity, surface structure, and structural inhomogeneities.

The elastic behaviour of a homogenous glass can be fully described by two independent moduli. The most commonly used elastic moduli are:

K = Modulus of compressibility or bulk modulus

G - Modulus of rigidity or shear modulus

E = Young's modulus related to the elongation of a glass under uniaxial tension.

μ = Poisson's ratio = ratio of lateral (contraction) to longitudnal strain (elongation) under uniaxial tensile stress.

From the view point of lattice dynamics K and G are the most fundamental moduli. For glass μ has a characteristic value, which in turn causes other moduli to show a characteristic relationship:

$\mu = 0.25$

$G \approx 0.4\ E$

$K \approx 0.67\ E$

Elastic moduli of some of glasses, measured by Kee[55] are given below.

Type	$\alpha(10^{-6}$ cm/cmF)	E(Psi x 10^{6})	μ	Thermal Shock Resistence °F
Soda Lime	5.1	10.48	0.20	117
Borosilicate	3.4	10.04	0.21	288
Aluminosilicate	2.7	12.46	0.25	243
Fused Silica	0.31	10.48	0.15	2250

A simple way of calculating the expected breaking stresses of a perfect solid is due to Orewan[56]. It is only a crude estimate but has the advantage of being applicable to all solids whatever the detailed nature of the interatomic forces. If we attempt to pull a perfect solid apart at absolute zero the

restraining forces between two adjacent atomic planes must vary with distance as shown in Figure II.1.

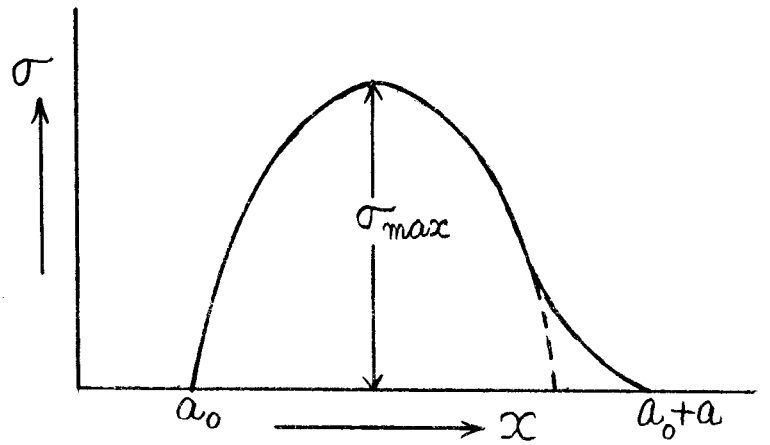

Fig. (II.I)

At equilibrium separation of the atomic planes a_o, the force is zero. It must rise to a maximum and then fall to zero. The exact form of the curve depends upon the nature of the inter-atomic forces. The area under the curve must represent the work of fracture. The work of fracture cannot be less than the surface energy of two new surfaces created when the solid breaks. A simple form to assume for variation of restraining force with distance is to write the stress σ as

$$\sigma = C \sin \frac{\pi}{a}(x - a_o) \tag{1}$$

when $(x - a_o)$ is very small

$$\frac{d\sigma}{dx/a_o} = C\pi\frac{a_o}{a}\cos\frac{\pi}{a}(x - a_o) \equiv E \tag{2}$$

where E is the Young's modulus of the solid

$$\therefore \quad C = \frac{E}{\pi} \frac{a}{a_0} \tag{3}$$

We do not know the value of 'a' which is a measure of the "range of interatomic forces". To evaluate 'a' following Orewan[56] we set the area under the curve equal to the surface energy of the two new surfaces created

$$\int_{a_0}^{a_0+a} \sigma \, dx = 2\gamma \tag{4}$$

where γ is the surface energy.

$$a = \frac{\pi\gamma}{C} \tag{5}$$

The theoretical breaking stress σ_{max} is given by the maximum value of σ in equation (1)

$$\sigma_{max} = C = \frac{E}{\pi} \cdot \frac{a}{a_0} = \sqrt{\frac{E\gamma}{a_0}} \tag{6}$$

'a' will be approximately equal to a_o, this gives a rough estimate of E, from equation (5)

$$a_0 = \frac{\pi^2 \gamma}{E} = 10\gamma/a_0$$

For silica glass $\gamma \approx 560$ ergs/cm^2 and $a_o \approx .5$ Å $= 5 \times 10^{-9}$ cm.

$$E = \frac{10 \times 560}{5 \times 10^{-9}} \text{ dynes/cm}^2 = 10^6 \text{ psi}$$

which is the right order of magnitude of the measured value. Using the experimental value of $E \approx 7 \times 10^{11}$ dynes/cm^2 we can estimate the maximum stress

$$\sigma_{max} = \frac{E}{\pi}$$
$$= 2 \times 10^{11} \text{ dynes/cm}^2$$
$$= 3 \times 10^6 \text{ psi}$$

This value for σ_{max} is very high. All commercially available glasses have a strength of only 25×10^3 psi. Even carefully prepared samples where special pains are taken to draw rods without making material contact with the surface, show a maximum tensile strength of only 4×10^5 psi. Griffith proposed that one can account for this notoriously low strength of glass by assuming the presence of submicroscopic crack like flaws as a normal characteristic of the glass. Because of the stress concentrating effect of these microcracks, the overall strength of the material is decreased. Removal of these cracks by etching or careful production of the material does increase its strength. In addition to these surface flaws Smekal assumed that the bulk of the glass also develops an extensive system of cracks with dimensions of the order of 10^{-6} cm. He describes this system of fissures or highly stressed regions within the glass as "natural inhomogenety of the glass". These flaws determine the stress distribution within the sample and also affect the

propagation of a crack, its forking and the brittleness of glass. Important experimental evidence for the presence of these voids comes from the observation of an increase in the E moduli with increasing temperature in glasses[55]. From this observation one may conclude that in glasses the number of bonds per unit cross section increases with heating.

In view of the aperiodicity and the heterogeneity of glasses, isolated measurements have little meaning. In spite of all the precautions taken to provide uniform test pieces the strength values scatter widely. This feature makes experimentation very difficult.

Kee[55] made a careful measurement of the mechanical properties of some glasses. Using this data on the mechanical properties one can calculate the susceptibility to thermally caused stresses. These stresses are of two types: steady-state stresses caused by temperature gradients within the glass part and transient stress caused by sudden heating or cooling. The magnitude of stresses resulting from thermal gradients depends on the restraints imposed on the sample part by the external mounting or by other portions of the glass part. When the glass part is completely constrained, the cooler side will be in tension and the maximum stress can be calculated with the formula:

$$\sigma_{max} = \frac{\alpha E \Delta T}{2(1-\mu)}$$

where ΔT is the difference in temperature, α linear expansion coefficient, μ - the Poisson's ratio and E is the Young's

modulus. Thermal shock from sudden cooling will cause more failure than from sudden heating, because cooling induces tensile stresses. These stresses increase proportionally with the expansion coefficient of the glass and in a direct but complex way with the thickness. Kee[55] measured the thermal shock resistance for BSC glass to be 240° F. Using his data we can calculate σ_{max}, which is;

$$\sigma_{max} = 5800 \text{ psi}$$

Thus the maximum thermally caused tensile stress that glass can withstand in cooling is 5800 psi. Tensile and compressive strengths of various glasses are listed in the International critical tables. Compressive strengths are higher by a factor of 10 to 15 than the tensile strength. In the laser induced mechanical damage, its the sudden heating which sets up compressive radial thermal stresses and oscillatory Hoop stresses which are both tensile and compressive. Thus the mechanical damage in this case is caused by the hoop stresses as scon as their tensile value exceeds the strength of the glass.

APPENDIX III

EVALUATION OF THE SCATTERING CROSS SECTION

In all theories of breakdown the electron lattice scattering cross section plays an important role. Various mathematical techniques have been employed in the treatment of the electron-lattice interaction.[41,57,60] The sources of interaction energy have been discussed by Frohlich and Seitz[57] who distinguish three possible contributions to it for the case in which the electron has insufficient energy to cause ionization from the valence band.

(i) Interaction with a dipolar field arising from the lattice vibrations of an ionic crystal considered as a lattice of point charges. Thus a longitudinal mode of vibration of such a lattice is a longitudinal wave of electric polarization.

(ii) Interaction with a dipolar field which arises from the distortion of the electron shells associated with the vibration of the lattice proper. This interaction is closely related to (i).

(iii) Interaction with a short range non-dipolar component of the field arising from the distortion of the electron shells.

In polar crystals all the three interactions occur, while in non polar crystals there are no dipolar field contributions.

Various models of crystals account differently for these three contributions. In the case of polar crystals, if the lattice is treated as a set of point charges each having the ionic charge and mass, only the interaction contribution (i) is considered and the distortion of the electron shells is neglected. This point charge approximation is good only when the most important processes considered involve short range polarization waves of the lattice. Another model of polar crystals considers the vibrations to be those of a continuum of known high and low frequency dielectric constant and lattice vibration frequencies. In this way interactions (ii) and (iii) are taken into account in a manner which leads to a good approximation when the most important processes involves polarization waves of long wavelength.

The general results obtainable from the application of perturbation theory are summarized below: Consider a single electron interacting with a dielectric medium which is represented by a set of harmonic oscillators whose angular frequency ω is a function of their wave number w. The hamiltonian may be written as

$$H = H_{electronic} + H_{lattice} + H_{interaction} \qquad (1)$$

If one confines attention to transitions in which only one quantum of lattice vibrational energy is absorbed or emitted the transition probability can be written as

$$P_w = \frac{2\pi}{\hbar} |M|^2 \delta(\xi) \qquad (2)$$

where w is the wave vector of the lattice oscillator involved in the transition, M is the matrix element of H_{int} between the initial and final states and

$$\xi = E_{k'} - E_k + (n'_w - n_w)\hbar\omega \qquad (3)$$

here k is the electron wave vector, $\hbar\omega$ the lattice quantum and n_w the average number of lattice quanta of wave vector w. The primed and the unprimed quantities refer to the initial and final states respectively. Conservation of energy is ensured by the δ-function. The square of the matrix element is given by

$$|M|^2 = G(w)\begin{Bmatrix} n_w \\ (n_w+1) \end{Bmatrix} \qquad (4)$$

for the cases in which wave number is conserved

$$\begin{aligned} k + w &= k' \quad \text{(absorption)} \\ k &= k' + w \quad \text{(emission)} \end{aligned} \qquad (5)$$

The function of G(w) depends on the interaction potential between the electron and the lattice vibrations. The interaction

constant G(w) has been calculated for two special models of polar crystals. In the continuum model the crystal is represented by a continuous dielectric medium of volume V with low and high frequency dielectric constants ϵ_o and ϵ_∞ and having a single angular frequency ω, which is independent of the wave number w for longitudinal polarization waves. Then G(w) as calculated by Frohlich, Pelzer and Zienan[58] is given by

$$G(w) = \frac{2\pi e^2 \hbar\omega}{V w^2} \left(\frac{1}{\epsilon_\infty} - \frac{1}{\epsilon_o}\right) \qquad (6)$$

This method of calculation should give satisfactory results for the long polarization waves (i.e. $w \ll a$, where a is the lattice constant).

In the point-charge model the lattice is represented by a discrete set of point charges alternately +e and -e with ionic masses M_+ and M_-. Frohlich[59] shows that

$$G(w) = \frac{2\pi^2 e^4 \hbar}{a^3 w^2 V M \omega} \qquad (7)$$

where M is the reduced mass given by $M = \left(\frac{1}{M_+} + \frac{1}{M_-}\right)^{-1}$. This form of interaction should be satisfactory for $w \sim a$. The relations 6 and 7 have the same functional dependence on w but due to the point charge model G(w) is about 3 times larger in (6) as compared with (7).

If the energy change per inelastic collision is much smaller than the electron energy we can define a relaxation time $\tau(E, T_o)$ for a conduction electron subject to collisions with the lattice by

$$\frac{k_x}{\tau(E,T_o)} = -\left(\frac{\partial k_x}{\partial t}\right)_{collision} = -\sum_w \left[\Delta k_x^a(w) P_w^a + \Delta k_x^e(w) P_w^e\right] \tag{8}$$

where x refers to some specified direction and $\Delta k_x^{a,e}$ is the mean change in k_x in one collision with oscillator w. In all cases the superscripts a and e refer to absorption and emission respectively. Now $\Delta k_x^{e,a}(w) = w \cos(k,w)_{e,a} \cos\theta$ as shown from Figure III.1. Using the conservation of energy we get

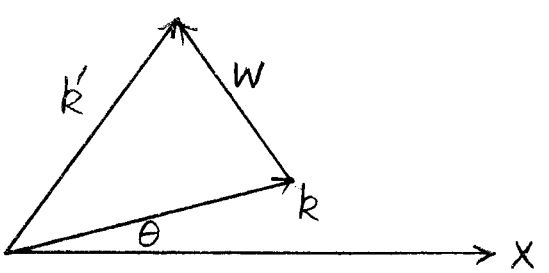

Fig. III.1

$$\frac{\Delta k_x^{e,a}(w)}{k_x} = -\frac{w^2}{2k^2} \pm \frac{mw}{\hbar k^2} \tag{9}$$

Using (2), (4) and (9) in (8) and reducing the sum to an integral

$$\frac{1}{\tau(E,T_0)} = \frac{V m}{4\pi k^3 \hbar^3}\left[\int w^3 G(w)\left\{1+\frac{2m\omega}{\hbar w^2}\right\}(1+n_w)dw\right.$$

$$\left.+\int w^3 G(w)\left\{1-\frac{2m\omega}{\hbar w^2}\right\} n_w\, dw\right]. \qquad (10)$$

where the integration in each case is over the appropriate region of lattice wavenumbers. A further simplification is possible for the case of high energy electrons. In this case the phonons which lead to large angle scattering will be those of large wavenumbers. In this case w ~ $\frac{1}{a}$ and

$$\frac{2m\omega a^2}{\hbar} \ll 1 \qquad (11)$$

Using (7) and (11) in (10) we obtain

$$\frac{1}{\tau(E,T_0)} = \frac{\pi m e^4}{2\hbar^2 a^3 M\omega k^3}\int w(1+2n_w)dw. \qquad (12)$$

The lower limit on w can be put equal to zero since the low wavenumbers do not appreciably contribute and the upper limit can be determined from the Debye condition

$$w_0 = (6\pi^2 N)^{1/3}$$

where N is the number of unit cells per unit volume. For alkali halides $N = \frac{1}{2a^3}$ where a is the nearest neighbour distance, so that

$$w_0 = \left(\frac{3\pi^2}{a^3}\right)^{1/3} \simeq \frac{\pi}{a} \qquad (13)$$

Such a large value of w_o can only be used as the upper limit of integration provided that the electron interacting with the phonon has sufficient energy to satisfy the requirement of conservation of momentum. This means that $k > \frac{w_o}{2}$ or in terms of energies $E > E_o$ where

$$E_0 = \frac{\hbar^2 w_0^2}{8m} \simeq \frac{\hbar^2}{32 m a^2} \qquad (14)$$

which is an energy of several electron volts. For $E > E_o$ the integration in (11) then gives

$$\frac{1}{\tau(E,T_0)} = \frac{\pi^3}{4\sqrt{2}} \frac{e^4 \hbar}{m^{1/2} M a^5 \omega E^{3/2}} \left\{1 + \frac{2}{e^{\frac{\hbar\omega}{k_0 T_0}} - 1}\right\} \qquad (15)$$

If $E < E_o$ then the upper limit in the integral is just 2k and

$$\frac{1}{\tau(E,T_0)} = \frac{\pi}{\sqrt{2}} \frac{m^{1/2} e^4}{\hbar M a^3 \omega E^{1/2}} \left\{1 + \frac{2}{e^{\hbar\omega/k_0 T_0} - 1}\right\} \qquad (16)$$

For the case of $E < E_o$, that is for low energy electrons it is more appropriate to use the expression (6) for G(w). The upper limit will still be 2k. Calculation of $\tau(E,T_o)$ for this case gives

$$\frac{1}{\tau(E,T_o)} = \left(\frac{m}{2E}\right)^{1/2} \cdot \frac{e^2\omega}{k}\left(\frac{1}{\epsilon_\infty} - \frac{1}{\epsilon_o}\right)\left\{1 + \frac{2}{e^{\frac{\hbar\omega}{k_o T_o}} - 1}\right\} \qquad (17)$$

Non Polar Crystals:

The treatment of the electron-lattice interaction is based on the work of Seitz[41] in which the interaction energy is introduced in the same way as in the conduction theory of metals using the deformable atom hypothesis. Considering the scattering of the electron to be the result of interaction with accoustical lattice modes only, adopting a linear relation between frequency and wavenumber

$$\omega = WS \qquad (18)$$

where s is the velocity of sound, and using perturbation theory in a way similar to the case of polar crystals yields for the transition probability

$$P_W^{e,a} = \frac{4\pi}{9} C^2 W \frac{\hbar}{MNVs} \begin{cases} (1+n_W)\delta(\xi) \\ n_W \delta(\xi) \end{cases} \qquad (19)$$

where C is the interaction constant (of order of 1 eV for many non polar crystals, M is the atomic mass and N the number of atoms per unit volume and ξ is given by (3). For the low energy electrons (of energy of order of several $k_o T_o$) the conservation of wavenumber will then permit interaction only with modes of low wave number. For such modes

$$n_W = \frac{k_o T_o}{\hbar W S} \tag{20}$$

Calculations similar to the previous cases show that the average relaxation time for an electron of energy E is given by

$$\frac{1}{\tau(E)} = \frac{4\sqrt{2}\, C^2 k_o T_o \, m^{3/2}}{9\pi \quad \hbar^4 s^2 \, M N} E^{1/2} \tag{21}$$

It should be noted that the use of perturbation theory is well justified for the case of slow electrons in non polar crystals but the value of the interaction constant is unknown.

Values of τ for three different electron energies are summarized in the table below

M O D E L	τ in units of 10^{-15} sec Electron energy		
	1 eV	2 eV	3 eV
Polar Crystals (High energy approximation)	2.81	4.14	4.74
Polar Crystals (Low energy approximation)	19.4	27.4	33.5
Continuum Model Phonon wave vector << a- -(lattice spacing)	24.9	36.0	43.1
Non Polar crystals Interaction constant C = 100 eV	2.3	1.63	1.56

BIBLIOGRAPHY

References are numbered and listed in the order in which they first appear in the text.

1. M. Hercher, J. Opt. Soc. Amer. 54, 563 (1964).
2. J. H. Cullom and R. W. Waynant, Appl. Optics 3, 989 (1964).
3. J. P. Budin and J. Raffy, Appl. Phys. Letters 9, 291 (1966).
4. D. W. Harper, Brit. J. Appl. Phys. 16, 751 (1965).
5. D. Olness, Appl. Phys. Letters 8, 283 (1966).
6. A. I. Akimov, L. I. Mirikin and N. F. Pilipetskii, Mechanica Polymerov 3, 493 (1967).
7. B. M. Ashkinadze, V. I. Vladimirov, V. A. Likhacher, S. M. Ryvkin, V. M. Salmanov and I. D. Yaroshetskii, Soviet Physics JETP 23 788(1966).
8. R. A. Miller and N. F. Borrelli, Appl. Optics 6, 165 (1967).
9. C. H. Conners and R. A. Thompson, J. Appl. Phys. 37, 3434 (1966).
10. R. Y. Chiao, C. H. Townes and B. P. Stoicheff, Phys. Rev. Letters 12, 592 (1964).
11. C. R. Giuliano, Appl. Phys. Letters 5, 137 (1964).
12. B. S. Sharma and K. E. Rieckhoff, Can. J. Phys. 45, 3781 (1967).
13. V. K. Rohatgi, J. Appl. Phys. 28, 951 (1957).
14. A. Gold and H. B. Bebb, Phys. Rev. Letters 14, 489 (1965).
15. Robert R. Johnston, J. Quant. Spectrosc. Radiat. Transfer 7, 815 (1967).
16. O. B. Firsov and M. I. Chibisov, Soviet Physics JETP 12, 1235 (1961).
17. J. K. Wright, Proc. Phys. Soc. 84, 41 (1964).
18. V. D. Frechette and Carl Cline, Interaction of Radiation with Solids, Edited by A. Bishay (Plenum Press New York, 1967).

19. H. Dupont, A. Donzel and J. Ernest, Appl. Phys. Letters 11, 271 (1967).

20. I. S. Sokolnikoff, Mathematical Theory of Elasticity (McGraw Hill Book Co., New York 1956).

21. M. Born and E. Wolf, Principles of Optics (The Macmillan Company, New York 1964).

22. M. Abraham and R. Becker, Electricity and Magnetism (Blackie, Ondon 1937).

23. H. B. Huntington, Solid State Physics 7, 213 (1958).

24. N. M. Kroll, J. Appl. Phys. 36, 34 (1965).

25. J. P. Budin, A. Donzel, J. Ernest and J. Raffy, Electronics Letters 3, 31 (1967).

26. A. I. Ritus and A. A. Manenkov, JETP Letters 6, 349 (1967).

27. B. M. Vul, Soviet Physics Solid State 3, 1644 (1962).

28. V. E. Culler and H. E. Rexford, Proc. IEEE 112, 1462, (1965).

29. T. V. Chang and C. K. Birdsall, Appl. Phys. Letters 5, 171, (1964).

30. V. S. Dneprovskii, D. N. Klyshiko and A. N. Penin, JETP Letters 3, 251 (1966).

31. E. M. Logothetics and P. L. Hartman, Phys. Rev. Letters 18, 581 (1967).

32. C. M. Verber and A. H. Adelman, J. Appl. Phys. 36, 1522 (1965).

33. A. Kats and J. M. Stevels, Phillips Res. Repts. 11, 115 and 156 (1956).

34. P. M. Sutton, J. Am. Cerm. Soc. 47, 188 (1964).

35. N. F. Mott and R. W. Gurney, Electronic Processes in Ionic Crystals 2nd ed. (Dover, New York)

36. L. D. Landau and E. M. Lifshitz, Quantum Mechanics (Addison-Wesley Publishing Co.)

37. L. V. Keldysh, Soviet Physics JETP 20, 1307 (1965).

38. P. E. Haworth and R. M. Bozorth, Physics 5, 15 (1934).

39. R. W. Minck and W. G. Rado, Physics of Quantum Electronics, P. L. Kelley et al Eds. (McGraw Hill Book Co., New York 1966).

40. P. Ehrenfest, Z. Physik 45 455, (1927).

41. F. Seitz, Phys. Rev. 76, 1376 (1949).

42. J. Vermeer, Physica 22, 1247 (1956).

43. N. S. Rudenko and V. I. Isvetkov, Soviet Physics-Tech. Physics 10, 1417 (1966).

44. R. V. D. R. Woolley and D. W. N. Stibbs, The Outer Layers of Stars (Oxford: Clarendon Press 1953).

45. Ya. B. Zeldovich and Yu. P. Raizer, Soviet Physics JETP 20, 772 (1965).

46. D. D. Ryutov, Soviet Physics JETP 20, 1472 (1965).

47. G. A. Askaryan and M. S. Rabinovich, Soviet Physics JETP 21, 190 (1965).

48. A. V. Phelps, Physics of Quantum Electronics (P. L. Kelley et. al Eds. McGraw Hill Book Co., New York 1966).

49. P. F. Browne, Proc. Phys. Soc. 86, 1323 (1965).

50. M. Young and M. Hercher, J. Appl. Phys. 38, 4393 (1967).

51. W. H. Zachariasen, J. Amer. Chem. Soc. 54, 3841 (1932).

52. K. H. Sun, J. Amer. Cerm. Soc. 30, 277 (1947).

53. G. Tammann and A. Rohmann, Z. Anorg u. allgem Chem. 183, 1 (1929).

54. B. E. Warren, J. Appl. Phys. 8, 645 (1937).

55. Herbert Kee, Product Engineering 32, 84 (1961).

56. E. Orewan, Report Progress in Physics 12, 185 (1949).

57. H. Fröhlich and F. Seitz, Phys. Rev. 79, 526 (1950).

58. H. Fröhlich, H. Pelzer and S. Zienau, Phil. Mag. 41, 221 (1950).

59. H. Fröhlich, Proc. Roy Soc. 160A, 230 (1937).

60. R. Stratton, Progress in Dielectrics 3, 233 (1961).

61. M. Young, M. Hercher and C. Wu, J. Appl. Phys 37, 4938 (1966).